UNIVERSIDADE FEDERAL DE MINAS GERAIS
Programa de Pós-Graduação em Engenharia Metalúrgica, Materiais e de Minas

Tese de Doutorado

Encruamento e Evolução Microestrutural do Alumínio Submetido à Compressão Multiaxial (MAC) Após ECAP

Autor: Cleber Granato de Faria
Orientador: Prof. Paulo Roberto Cetlin
Coorientadora: Profª. Maria Teresa Paulino Aguilar

Fevereiro/2019

Cleber Granato de Faria

Encruamento e Evolução Microestrutural do Alumínio Submetido à Compressão Multiaxial (MAC) Após ECAP

Tese apresentada ao Programa de Pós-Graduação em Engenharia Metalúrgica, Materiais e de Minas da Escola de Engenharia da Universidade Federal de Minas Gerais, como requisito parcial para obtenção do Grau de Doutor em Engenharia Metalúrgica, Materiais e de Minas.

Área de Concentração: Ciência e Engenharia de Materiais.

Orientador: Prof. Paulo Roberto Cetlin
Coorientadora: Profª. Maria Teresa Paulino Aguilar

Belo Horizonte
Universidade Federal de Minas Gerais
Escola de Engenharia
2019

Faria, Cleber Granato.
F224e Encruamento de Evolução Microestrutural do Alumínio submetido à Compressão Multiaxial (MAC) após ECAP [manuscrito] / Cleber Granato Faria. – 2019.
xii, 32 f., enc.

Orientador: Paulo Roberto Cetlin.
Coorientadora: Maria Teresa Paulino Aguilar.

Tese (doutorado) - Universidade Federal de Minas Gerais, Escola de Engenharia.

Inclui anexos e bibliografia.

1. Engenharia metalúrgica - Teses. 2. Microestrutura - Teses. 3. Metais - Teses. 4. Ligas (Metalurgia) – Teses. 5. Metais -- extrusão – Teses. I. Cetlin, Paulo Roberto, 1946-. II. Aguilar, Maria Teresa Paulino. III.Universidade Federal de Minas Gerais.Escola de Engenharia.IV.Título.

CDU: 669(043)

DEDICATÓRIA

À Giane, Ana Clara, Cesar e aos meus pais,
pelo apoio e carinho dados a mim durante esta etapa.

AGRADECIMENTOS

Aos orientadores e amigos *Paulo Roberto Cetlin* e *Maria Teresa Paulino Aguilar*, que compartilharam comigo seus conhecimentos, com muita generosidade, permitindo a realização deste trabalho.

Aos amigos *Lucas, Bruno, Gabriela, Daniel, Pedro Malaquias. Pedro Henrique e Natanael* pela colaboração nos experimentos durante a realização deste trabalho.

À Novelis do Brasil Ltda através do Remelt Process Leader Lúcio Carlos Murta Junior pela doação do alumínio usado no estudo.

SUMÁRIO

1. INTRODUÇÃO 1

1.1 CONTEXTUALIZAÇÃO, MOTIVAÇÃO E ORIGINALIDADE 1
1.2 OBJETIVO 3
1.3 MATERIAL E MÉTODOS 4
1.4 REFERÊNCIAS BIBLIOGRÁFICAS 6

2. ARTIGO 1 9

2.1 TITLE E ABSTRACT 10
2.2 INTRODUCTION 10
2.3 EXPERIMENTAL 12
2.4 RESULTS AND DISCUSSION 14
2.5 CONCLUSIONS 16
2.6 ACKNOWLEDGMENTS 17
2.7 REFERENCES 17

3. ARTIGO 2 20

3.1 TITLE E ABSTRACT 21
3.2 INTRODUCTION 21
3.3 EXPERIMENTAL 22
3.4 RESULTS AND DISCUSSION 23
3.5 CONCLUSIONS 28
3.6 ACKNOWLEDGMENTS 28
3.7 REFERENCES 28

4. CONCLUSÕES 30

5. SUGESTÕES PARA TRABALHOS FUTUROS 31

6. ANEXOS 32

LISTA DE FIGURAS

Figura 1.1 – Etapas experimentais. 5
Figure 2.1 – ECAP and compression testing in the present paper: (a) coordinate axes and direction of monotonic compression and (b) sequence of compressions in MAC processing. 13
Figure 2.2 – Stress – strain curves for the monotonic compression of the **An**, **An+ECAP** and **An+ECAP+MAC** materials, and for MAC in the ECAPed material. . 15
Figure 3.1 – OIM images for specimens in the conditions: (a) **An**, (b) **An+ECAP**, (c) **An+ECAP+LSA-MAC** and (d) **An+ECAP+LSA-MAC+COMP**. 24
Figure 3.2 – Grain boundary characteristics and grain disorientation distributions for specimens: (a, b) **An**, (c, d) **An+ECAP**, (e, f) **An+ECAP+LSA-MAC** and (g, h) **An+ECAP+LSA-MAC+COMP**. 26
Figure 3.3 – TEM images for the following conditions: (a, b) **An+ECAP**, (c, d) **An+ECAP+LSA-MAC** and (e, f) **An+ECAP+LSA-MAC+COMP**. 27

RESUMO

A crescente necessidade de materiais com propriedades multifuncionais tem motivado o desenvolvimento de novas ligas e técnicas de processamento. Dentre esses materiais, destacam-se os materiais de alta resistência mecânica obtidos por meio de técnicas de deformação plástica severa (*Severe Plastic Deformation*, SPD). Dentre estas técnicas, duas importantes são a extrusão angular em canais iguais, (*Equal Channel Angular Pressing*, ECAP) e a compressão multiaxial, (Multi-Axial Compression, MAC). A principal vantagem destas técnicas é a possibilidade do processamento de amostras com grandes dimensões, o que permitiria sua aplicação comercial. Porém, o aumento da resistência mecânica por deformação plástica geralmente é conseguido em detrimento da ductilidade, que é uma importante propriedade associada aos processos de conformação mecânica. Estudos sobre o comportamento mecânico de materiais submetidos a deformações multiaxiais mostram que materiais assim processados podem encruar ou amaciar, dependendo da condição inicial e/ou do incremento de deformação utilizado. Observa-se também, que além do amaciamento, o MAC pode aumentar a taxa de encruamento em materiais pré-encruados. Desta forma, o MAC poderia ser utilizado para a recuperação de parte da ductilidade perdida por materiais submetidos à ECAP e permitir que estes materiais possam ter maior aplicação. Com o objetivo de estudar a influência do MAC no comportamento de materiais pré-encruados por SPD, analisou-se, neste trabalho, o efeito da compressão multiaxial com baixa amplitude de deformação (0,075), no desempenho mecânico do alumínio comercialmente puro (99,77%), após pré-deformação por um passe de ECAP. Os resultados indicaram que o material amaciou após o MAC e recuperou parte da capacidade de encruamento perdida no pré-encruamento. Este comportamento estaria relacionado à estabilização da estrutura de deslocações desenvolvida pelo passe de ECAP em uma configuração com maior fração de contornos de alto ângulo (*High Angle Grain Boundaries*, HAGB).

ABSTRACT

The growing need for materials with multifunctional properties has motivated the development of new alloys and processing techniques. Among these materials, the high strength ones obtained via SPD (Severe Plastic Deformation) stand out. The two most important SPD techniques are ECAP (Equal Channel Angular Pressing) and MAC (Multi-Axial Compression) due to the possibility of processing industrial sized samples, which would allow commercial applications. However, the strength gained by processing is usually accompanied by a ductility loss, which is necessary for further metal forming operations. It has been shown that the mechanical behavior of materials submitted to multi-axial deformation can either work harden or soften. The expected behavior depends on the initial condition and the strain amplitude employed. It was also observed that MAC is capable of increasing work hardening capabilities of previously deformed materials. Therefore, MAC could be used to recover the lost ductility of materials previously submitted to ECAP, further increasing its applications. The present research main goal was to evaluate the influence of low strain amplitude (0.075) MAC on the mechanical behavior of commercial pure aluminum samples (99.97%) previously processed by one ECAP step. The results pointed out that the material softened and partially recovered its work hardening capability after MAC processing. This behavior was attributed to the stabilization of the dislocation structure developed during ECAP to a predominately HAGB (High Angle Grain Boundaries) configuration.

ESTRUTURA DA TESE

Esta tese está organizada em capítulos.

No capítulo 1, é apresentada a contextualização do tema, assim como a motivação, a originalidade e os objetivos do estudo. Também são descritos o material e métodos adotados.

Nos capítulos 2 e 3 são apresentados os dois artigos extraídos do estudo realizado, publicados em periódicos Qualis A1 da Engenharia II. Para facilitar a leitura, não foi adotada a formatação original exigida pela revista: alterou-se o tamanho da fonte, o espaçamento entre linhas e o número de colunas.

Nos capítulos 4 e 5 são apresentadas as conclusões e sugestões para trabalhos futuros, respectivamente.

Nos Anexos são apresentados os artigos como publicados.

1. INTRODUÇÃO

1.1 Contextualização, Motivação e Originalidade

A necessidade do mundo contemporâneo por materiais com propriedades diferenciadas tem exigido o desenvolvimento de novas ligas ou de técnicas de processamento [1]. Dentre estes materiais, destacam-se o alumínio e suas ligas devido à aparência, baixa massa específica e resistência à corrosão [2]. Entre as técnicas que podem ser utilizadas no melhoramento das propriedades do alumínio e suas ligas, estão os processamentos de deformação plástica severa (*Severe Plastic Deformation*, SPD) [1]. Estas técnicas se caracterizam pela imposição de elevadas deformações nos materiais sem mudanças significativas nas dimensões iniciais dos corpos de prova, promovendo assim a possibilidade do reprocessamento dos mesmos [3, 4]. Esta elevada deformação promove o aumento da resistência (σ) devido à redução do tamanho médio do grão (d), que promove o aumento das interações entre as deslocações e os contornos de grão [5]. Dentre as técnicas de deformação plástica severa, uma das mais importantes e mais utilizada é a extrusão angular em canais iguais (*Equal Channel Angular Pressing*, ECAP) [5, 6], que consiste em submeter o material processado a grandes deformações, forçando sua passagem em canais de seções transversais iguais que se interceptam formando um ângulo entre si [7-9]. O aumento da resistência mecânica de materiais geralmente é conseguido em detrimento de sua ductilidade [1], que é uma importante propriedade associada aos processos de conformação mecânica. Algumas técnicas têm sido propostas para amenizar o problema da baixa ductilidade de materiais submetidos a SPD. Dentre elas pode-se destacar a distribuição de tamanho de grão bimodal [10-12] e a introdução de nano precipitados [13, 14]. No caso das ligas de alumínio, a adição de um alto teor de Zn, também, contribuiria para a melhoria da ductilidade [15]. Porém, estas estratégias envolvem aspectos complexos em relação à microestrutura e composição.

Estudos sobre o comportamento mecânico de materiais submetidos a deformações multiaxiais mostram que materiais assim processados podem amaciar ou encruar dependendo da condição inicial (recozido ou encruado) e do incremento de deformação

utilizado [16-19]. Dentre estas técnicas de deformação multiaxial destaca-se a compressão (*Multi-Axial Compression*, MAC) também conhecidas como forjamento multidirecional (*Multi-Directional Forging*, MDF), que se caracteriza pela compressão sequencial do material nas três direções ortogonais entre si com incrementos constantes de deformação, sendo que essa compressão pode ser repetida até que se obtenham grandes deformações totais [20]. Estudos sobre o comportamento de materiais metálicos pré-encruados por técnicas de processamento SPD submetidos a ensaios de fadiga de baixo ciclo (*Low Cicle Fadigue*, LCF) mostram que estes, como os materiais pré-deformados por métodos convencionais, também podem apresentar amaciamento dependendo da condição inicial e do incremento de deformação [21-27]. Desta forma, a aplicação da compressão multiaxial em materiais submetidos à ECAP poderia reestabelecer parte da ductilidade perdida pelo processamento de deformação plástica severa. Não foram encontrados estudos na literatura sobre este processamento. O presente trabalho avaliou a influência do MAC no comportamento mecânico e na evolução microestrutural de amostras de alumínio pré-deformadas por ECAP.

1.2 Objetivo

O objetivo geral deste trabalho foi analisar a influência da compressão multiaxial (*Multi-Axial Compression*, MAC) no comportamento mecânico e na microestrutura de amostras de alumínio comercialmente puro, recozidas e submetidas primeiramente a um passe de ECAP. Para isto, os seguintes objetivos específicos tiveram que ser atingidos:

1- avaliar o comportamento mecânico das amostras recozidas e processadas por um passe de ECAP;
2- avaliar o comportamento mecânico das amostras recozidas, processadas por ECAP e submetidas à compressão multiaxial (MAC);
3- avaliar a evolução microestrutural desenvolvida pelas amostras processadas por ECAP e compressão multiaxial (MAC);
4- propor uma nova técnica que alterne duas metodologias de SPD já consagradas, para melhorar as propriedades mecânicas dos materiais processados.

1.3 Material e Métodos

Neste estudo, essencialmente experimental, foi utilizado o alumínio comercialmente puro (99,77% Al, 0,15% Fe, 0,06 Si). No fluxograma da figura 1.1 é apresentado de forma esquemática os procedimentos experimentais assim como os artigos gerados pelo estudo. O material foi recebido no estado bruto de fusão. Para a eliminação desta estrutura inicial, o alumínio foi submetido a um passe de ECAP e recozimento. Parte das amostras recozidas foi submetida a ensaio de tração ou compressão, o restante a mais um passe de ECAP e posteriormente a compressão uni ou multiaxial. Ensaios de compressão também foram realizados nas amostras processadas por MAC. Todos estes ensaios foram realizados para a caracterização do comportamento mecânico das condições de processamento estudadas neste trabalho (recozido, recozido + ECAP, recozido + ECAP + MAC e recozido + ECAP + MAC + compressão). Estes resultados foram utilizados para a escrita do artigo I "*Increasing the work hardening capacity of equal channel angular pressed (ECAPed) aluminum through multi-axial compression (MAC)*". A caracterização microestrutural das condições citadas acima foi realizada por técnicas de microscopia eletrônica: analise por Difração de Elétrons por Retroespalhamento (*Electron BackScattered Diffraction*, EBSD) e Microscopia eletrônica de transmissão (*Transmission Electron Microscopy*, TEM). Os resultados obtidos por estas análises juntamente com os obtidos por medidas de microdureza foram utilizados na confecção do Artigo II "*Microstructural evolution in the low strain amplitude multi-axial compression (LSA-MAC) after equal channel angular pressing (ECAP) of aluminum"*.

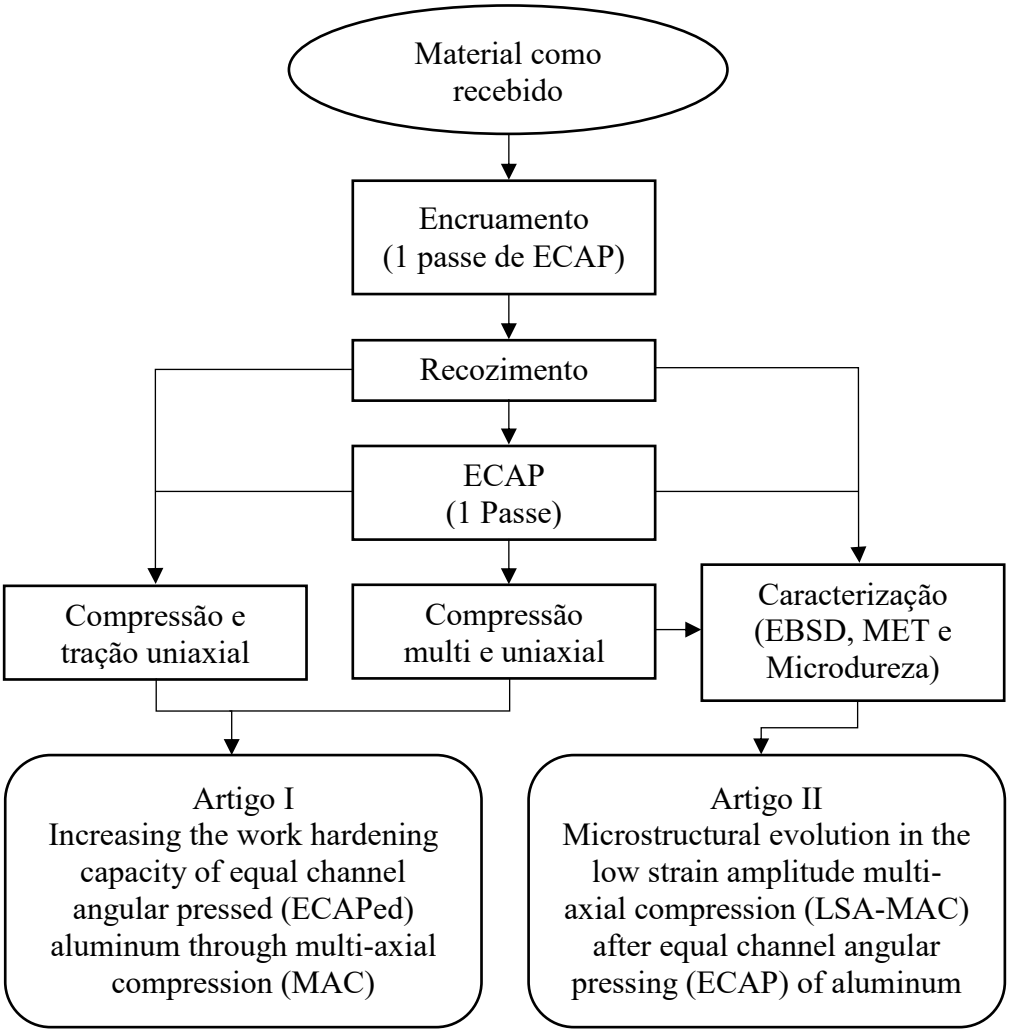

Figura 1.1 – Etapas experimentais.

1.4 Referências bibliográficas

[1] I. Sabirov, M.Y. Murashkin, R.Z. Valiev, Nanostructured aluminium alloys produced by severe plastic deformation: New horizons in development, Mater. Sci. Eng. A, 560 (2013), pp. 1-24.

[2] ASM Handbook. Properties and selection: Nonferrous alloys and special-purpose materials. 10th ed. Ohio: American Society for Metals - ASM International, 2 (1990).

[3] R.Z. Valiev, R.K. Islamgaliev, I.V. Alexandrov, Bulk nanostructured materials from severe plastic deformation, Prog. Mater. Sci., 45 (2000), pp. 103-189.

[4] A.P. Zhilyaev, T.G. Langdon, Using high-pressure torsion for metal processing: Fundamentals and applications. Prog. Mater. Sci., 53 (2008), pp. 893-979.

[5] T.G. Langdon, Twenty-five years of ultrafine-grained materials: Achieving exceptional properties through grain refinement. Acta Mater. 61 (2013), pp. 7035–7059.

[6] Y. Estrin, A. Vinogradov, Fatigue behaviour of light alloys with ultrafine grain structure produced by severe plastic deformation: an overview. Int. J. Fat., 32 (2010), pp. 898-907.

[7] R.Z. Valiev, T.G. Langdon, Principles of equal-channel angular pressing as a processing tool for grain refinement, Prog. Mater. Sci., 51 (2006), pp. 881-981.

[8] T.G. Langdon, The principles of grain refinement in equal-channel angular pressing. Mater. Sci. Eng. A, 462, (2007), pp. 3-11,.

[9] E.A. El-Danaf, Mechanical properties and microstructure evolution of 1050 aluminum severely deformed by ECAP to 16 passes. Mater. Sci. Eng. A, 487 (2008), pp. 189-200.

[10] G.J. Fan, H. Choo, P.K. Liaw, E.J. Lavernia, Plastic deformation and fracture of ultrafine-grained Al–Mg alloys with a bimodal grain size distribution, Acta Mater., 54 (2006), pp. 1759-1766

[11] B.Q. Han, J.Y. Huang, E.J. Zhu, E.J. Lavernia, Strain rate dependence of properties of cryomilled bimodal 5083 Al alloys, Acta Mater., 54 (2006), pp. 3015-3024.

[12] Y. Wang, M. Chen, F. Zhou, E. Ma, High tensile ductility in a nanostructured metal, Nature, 419 (2002), pp. 912-915.

[13] S. Cheng, Y.T. Zhao, E. Zhu, Optimizing the strength and ductility of fine structured 2024 Al alloy by nano-precipitation, Acta Mater., 55 (2007), pp. 5822-5832.

[14] M. Hockauf, L.W. Meyer, B. Zillman, M. Hietschold, S. Schultze, L. Krueger, Simultaneous improvement of strength and ductility of Al–Mg–Si alloys by combining equal-channel angular extrusion with subsequent high-temperature short-time aging, Mater. Sci. Eng. A, 503 (2009), pp. 167-171.

[15] R.Z. Valiev, M.Y. Murashkin, A. Kilmametov, B. Straumal, N.Q. Chinh, T.G. Langdon, Unusual super-ductility at room temperature in an ultrafine-grained aluminum alloy, J. Mater. Sci., 45 (2010), pp. 4718-4724.

[16] L.F. Coffin, J. F. Tavernelli, The cyclic straining and fatigue of metals. Trans Metall Soc AIME, 215 (1959), pp. 794-807.

[17] C.E. Feltner, C. Laird, Cyclic stress-strain response of FCC metals and alloys-I Phenomenological experiments. Acta Met., 15 (1967), pp. 1621-1632.

[18] P.E. Armstrong, J.E. Hockett, O.D. Sherby, Large strain multidirectional deformation of 1100 aluminum at 300 K, J. Mech. Phys. Solids, 30 (1982), pp. 37-58.

[19] E.C.S. Corrêa, M.T.P. Aguilar, E.M.P. Silva, P.R. Cetlin, The effect of sequential tensile and cyclic torsion straining on work hardening of steel and brass. J. Mater. Proc. Tech. 142 (2003), pp. 282-288.

[20] T. Sakai, A. Belyakov, R. Kaibyshev, H. Miura, J.J. Jonas, Dynamic and post-dynamic recrystallization under hot, cold and severe plastic deformation conditions, Prog. Mater. Sci., 60 (2014), pp. 130-207.

[21] A. Vinogradov, Y. Kaneko, K. Kitagawa, S. Hashimoto, V. Stolyarov, R. Valiev, Cyclic response of ultrafine-grained copper at constant plastic strain amplitude. Scr. Mater., 36 (1997), pp. 1345-1351.

[22] S.R. Agnew, J.R. Weertman, Cyclic softening of ultrafine grain copper. Mater. Sci. Eng. A, 244 (1998), pp. 145-153.

[23] S. Malekjani, P.D. Hodgson, P. Cizek, I. Sabirov, T.B. Hilditch, Cyclic deformation response of UFG 2024 Al alloy. Int. J. Fat., 33 (2011), pp. 700-709.

[24] S. Malekjani, P.D. Hodgson, P. Cizek, T.B. Hilditch, Cyclic deformation response of ultrafine pure Al. Acta mater., 59 (2011), pp. 5358-5367.

[25] R. Zhu, Y.J. Wu, W.Q. Ji, J.T. Wang, Cyclic softening of ultrafine-grained AZ31 magnesium alloy processed by equal-channel angular pressing. Mater. Let., 65 (2011), pp. 3593-3596.

[26] S. Malekjani, P.D. Hodgson, N.E. Stanford, T.B. Hilditch, Shear bands evolution in ultrafine-grained aluminium under cyclic loading. Scr. Mater., 68 (2013), pp. 821-824.

[27] T. Niendorf, A. Böhner, H.W. Höppel, M. Göken, R.Z. Valiev, H.J. Maier, Comparison of the monotonic and cyclic mechanical properties of ultrafine-grained low carbon steels processed by continuous and conventional equal channel angular pressing. Mater. Des., 47 (2013), pp. 138-142.

2. Artigo 1

2.1 Title e Abstract

Increasing the work hardening capacity of equal channel angular pressed (ECAPEd) aluminum through multi-axial compression (MAC)

The low strength of commercial purity aluminum can be increased by solid solution, precipitation/aging, work hardening and grain size decrease. The latter has been extensively studied utilizing Severe Plastic Deformation (SPD), leading, however, to a negligible final uniform tensile ductility of the material due to its low or negative work hardening rates. Microstructural and compositional techniques have been used to partially circumvent this problem. Multi-axial compression (MAC) of previously compressed Aluminum can soften the material and lead to increased work hardening capacity under ulterior monotonic compression. In the present research, MAC was applied to Aluminum after SPD employing Equal Channel Angular Pressing (ECAP). The material softened after MAC, and its ulterior compression evolved with a much higher work hardening rate than in the absence of MAC, thus opening a new possibility of mechanically increasing the work hardening capacity and uniform ductility of Aluminum (and other materials) after ECAP.

Keywords: equal channel angular pressing (ECAP), multiaxial compression (MAC), work hardening

2.2 Introduction

Aluminum is widely available and presents, low cost, light weight, corrosion resistance, ductility and attractive finish. High purity aluminum displays however a yield strength of only about 10 MPa [1], which can be increased through solid solution, precipitation/aging, work hardening and grain refinement. The latter has led to many researches in order to obtain exceptionally small grain sizes (below 1μm) through Severe Plastic Deformation (SPD) processes [2].

SPD has been achieved through ECAP (Equal Channel Angular Pressing) [3], ARB (Accumulative Roll Bonding) [4], HPT (High Pressure Torsion) [5], and MAC (Multi Axial Compression, also known as Multi Axial Forging - MDF) [6-10]. ECAP is attractive because it can produce large samples and is adaptable to continuous and high output processes [11], leading to end products useful for structural purposes.

The material uniform ductility after SPD is very limited in the low temperature regime, for stress states with tensile components such as sheet forming, bending and simple tension [12]. This is caused by the negligible or negative work hardening rates observed in the monotonic deformation of materials after SPD [2]. Some techniques have been suggested in order to alleviate this problem: (i) a bi-modal grain size distribution [13-15] (ii) the introduction of nano-precipitates in the material [16, 17] and (iii) high Zn contents in Aluminum [6]. These approaches involve complex microstructural and compositional aspects.

An early study connected to MAC in Aluminum was performed by Armstrong et al. [18], involving strain amplitudes from 0.075 to 0.33 at room temperature and comparing the results with those for monotonic compression. This contrasts to more recent analyses, [7-9, 19] where strain amplitudes range from 0.4 to 0.6, homologous temperatures vary from 0.1 to 0.5 and there is no comparison with monotonic compressions. Armstrong et al. [18] report that MAC led to: (i) lower work hardening and strength than monotonic compression, (ii) lower work hardening as the strain amplitude decreased, (iii) softening of monotonically compressed material when submitted to a subsequent MAC, provided that the strain amplitude in MAC were lower than the initial monotonic strain and (iv) if the material thus softened underwent a monotonic compression again, it would work harden at a higher rate than for full previous monotonic compression, for the same levels of deformation.

The above findings suggest that the post-SPD work hardening capacity and consequent uniform tensile ductility of materials would increase through the application of MAC with a strain amplitude lower than the applied monotonic SPD deformation, but that some strength loss is also expected. This approach is simpler than the microstructural and

compositional aspects already mentioned [6, 13-17] utilized in order to increase the post-SPD ductility of the material. It should be remembered that MAC does not change the dimensions of the initial material, and thus the work hardening increase can be viewed as available in the pre-MAC treated material.

The present paper presents experimental results concerning the strength and work hardening behavior of commercial purity aluminum under monotonic compression after one ECAP pass followed by a limited number of low strain amplitude MAC. As predicted, the material softened after MAC and displayed high work hardening rates in the final monotonic compression step. No similar investigation was found in the literature.

2.3 Experimental

The material was commercial purity cast aluminum (Al-99.77, Fe-0.15, Si-0.06 wt%) in cylinders 150 mm in diameter. Samples 15.8 x 15.8 x 100 mm³ were machined from this bar, with the long dimension parallel to the cylinder axis. These were deformed and annealed (hereafter referred to as **An** material) in order to break the as-cast initial structure; deformation involved one ECAP pass with channels at a 90º angle and sections of 15.9 x 15.9 mm^2, imposing a strain of $\varepsilon \approx 1.15$ [20], at room temperature and at ≈ 20 mm/min; the die/specimen interface was lubricated with molybdenum disulfide. The processed samples were annealed at 623 K for 7200s.

Monotonic compression and tension tests were performed in the **An** material, utilizing compression specimens with cross-section of 16.5 x 16.5 mm^2 and a height of 28.0 mm (height/width = 1.7) and tension specimens 35mm long and 5.0 mm in diameter, both lying along the X direction in Figure 2.1a, which was also the compression and tension direction. The compression die/specimen interfaces were lubricated with molybdenum disulfide paste, and testing was interrupted for every $\varepsilon \approx 0.1$ increment for interface re-lubrication, up to a total axial strain of $\varepsilon \approx 2.0$. Following Armstrong's [18] recommendations, specimens were re-machined back to the initial height/width ratio of 1.7 after deformations of $\varepsilon \approx 0.7$, in order to avoid excessive specimen distortions.

The annealed material ("**An**" material) was submitted to another ECAP pass ("**An+ECAP**" material) identical to the above described one, and performed along the "X" direction in Figure 2.1a. MAC was performed in the **An+ECAP** material ("**An+ECAP+MAC"** material). The specimens had the dimensions: 13.00 (direction X), 12.06 (direction Y) and 12.52 (direction Z) mm³, with a strain amplitude $\varepsilon \approx 0.075$. The interface between the compression die and the specimen was lubricated with molybdenum disulfide. Compressions sequence followed the X, Z and Y directions (Figure 2.1b). For all compression steps in an isotropic material deforming homogeneously, the direction under compression had (i) an initial length of 13.00 mm after the previous $\varepsilon \approx 0.075$ straining in an orthogonal direction, and (ii) underwent a decrease in length of 0.94 mm. MAC was performed for 4 cycles (a total of 12 compressions), totaling an external strain of $\varepsilon \approx 0.9$. According to Armstrong [18] this leads to approximately 50% of the total possible softening through MAC in the **An+ECAP** material, considered as a reasonable goal in terms of final uniform ductility without an excessive loss of strength of the material.

An+ECAP+MAC specimens were submitted to monotonic compression along the X axis, in order to evaluate its post-MAC work hardening and strength.

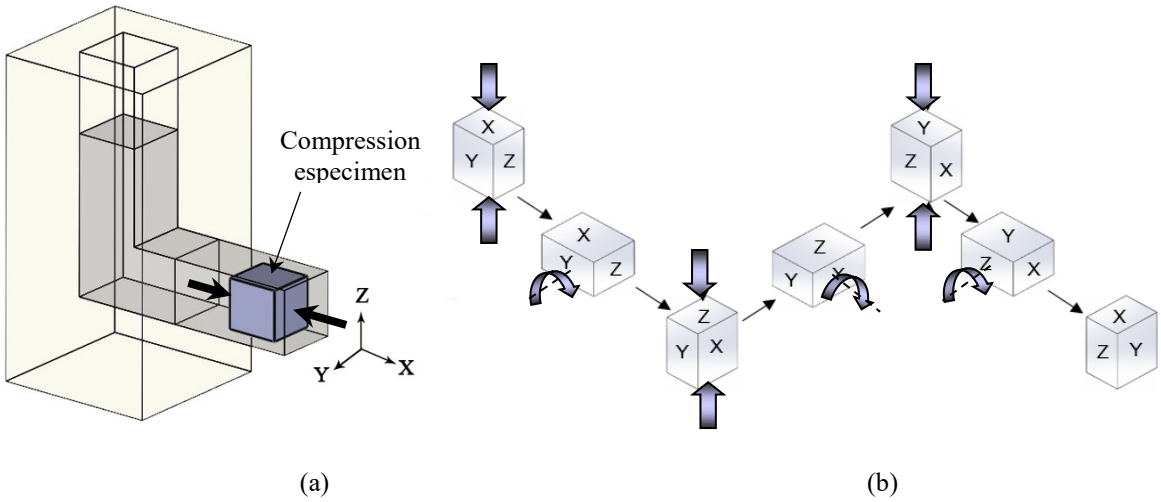

Figure 2.1 – ECAP and compression testing in the present paper: (a) coordinate axes and direction of monotonic compression and (b) sequence of compressions in MAC processing.

All testing was performed in duplicate in an INSTRON 5582 universal testing machine, at a crosshead speed of 0.005 mm/s. No remarkable differences were observed when comparing the results obtained for both sets of specimens.

2.4 Results and discussion

Figure 2.2 displays the stress-strain curves in monotonic compression for the **An**, **An+ECAP** and **An+ECAP+MAC** materials along direction X, as well as in the MAC for the **An+ECAP** material.

The stress-strain curve in the first compression of the **An+ECAP** material (along direction X) displays an initial peak ("spike") above the monotonic compression curve, followed by negative work hardening, similarly to the "cross-test effects" reported by Beyerlein et al. [21] for 99.99wt%Al. This is surprising, since the present post-ECAP compression in the X direction corresponds to a situation where slip in the shearing plane in ECAP is reversed on further compression, and should lead to Beyerlein's "reversed test effects" and no initial spike. El-Danaf's [22] results for 1050 Aluminum also displayed a "spike effect" but lower in relation to the present one. It is suggested that simple compression after ECAP, along the present "X" direction, can also lead to the activation of slip systems not previously activated during ECAP, similarly to the situation in "cross-test-effects" [21].

The observation of the stress-strain curves displayed in Figure 2.2 for the individual deformation steps during MAC indicates small variations in strain amplitude of the various steps, as well as situations where the initial parts of the curves display low levels of stress (see, e.g., the curve in the "Z" direction of the last MAC cycle). These phenomena are connected to lateral bulging of the samples in the previous deformation step. As the specimen is rotated and compressed, the initial part of the stress-strain curve corresponds to the "flattening" of the specimen surface by the compression platen. This also causes small errors in the average strain in the deformation step, since compression actually begins when the top of the specimen bulge contacts the compression platen. Similar bulging and consequent strain heterogeneity problems during MAC have been

recently reported [9]. Armstrong et al. [18] also mention bulging problems, but state that specimen re-machining was necessary only after a total strain of 0.7 was reached. The use of dies in constrained MAC practically eliminates bulging problems [23], and thus seems to be a more convenient method for MAC than the current free compression.

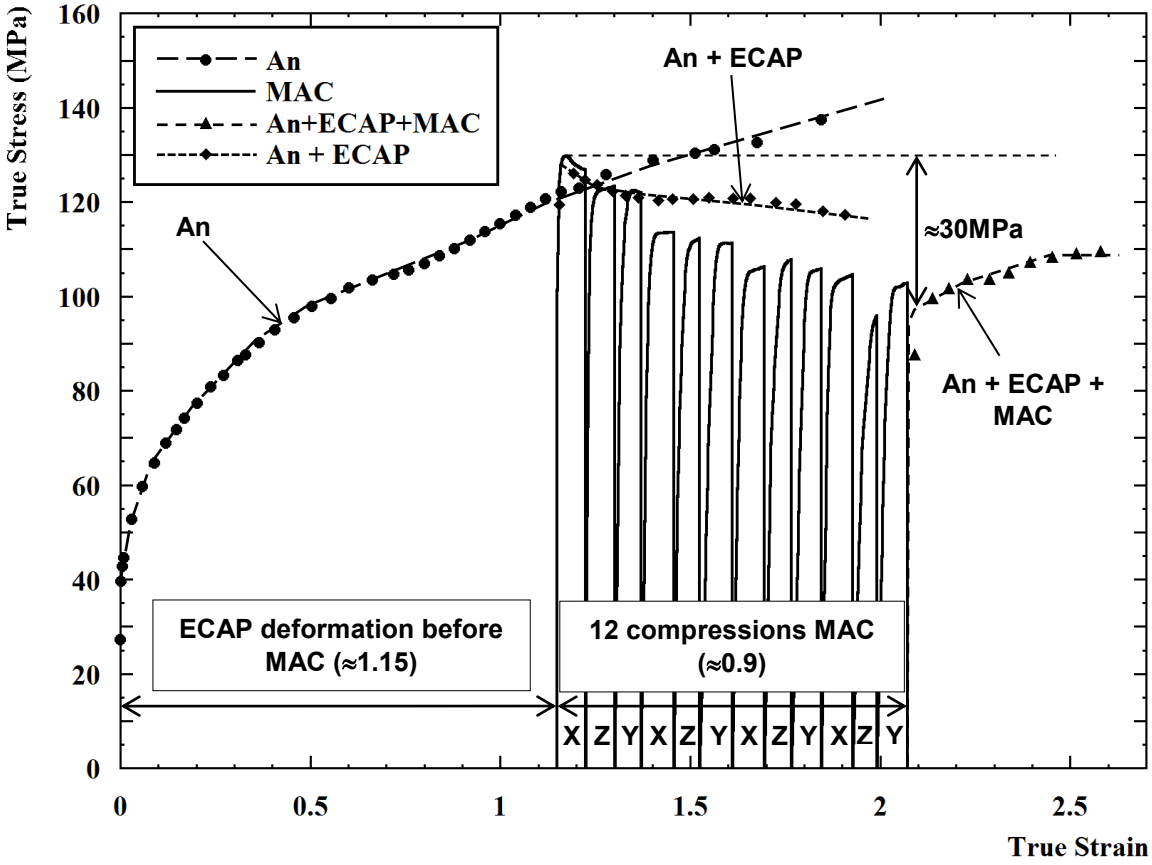

Figure 2.2 – Stress – strain curves for the monotonic compression of the **An**, **An+ECAP** and **An+ECAP+MAC** materials, and for MAC in the ECAPed material.

Figure 2.2 indicates that MAC caused a higher softening in the **An+ECAP** material than the monotonic compression along the X axis. The work hardening in the monotonic compression of the **An+ECAP+MAC** material is positive and obviously higher than the negative work hardening for the **An+ECAP** material, extrapolated to the straining interval of ≈ 2.1 to ≈ 2.6. Since MAC does not change the dimensions of the ECAPed material, the situation can be viewed as a direct increase in the work hardening capacity of the **An+ECAP** material.

Necking (and thus the uniform strain ε_u) in tensile testing occurs when $\theta = (d\sigma/d\varepsilon) / \sigma = 1$ [24]. The variation of θ with strain was evaluated for the monotonic compression and tension of the **An** material and for the **An+ECAP+MAC** materials. For compression and tension, $\theta = 1$ for $\varepsilon_u \approx 0.21$ to ≈ 0.23; all compressive strains above this strain range lead to immediate necking and to very low uniform strains under further tensile testing. This is the post-ECAP situation (strain of $\approx$ 1.15), where θ for monotonic compression becomes negative for very small strains (see the compression curve for the **An+ECAP** material). The same analysis for the **An+ECAP+MAC** material indicated that the $\theta = 1$ condition is reached for $\varepsilon_u \approx 0.043$, which is higher than that reported for Ti-13Nb-13Zr [24] as a consequence of the use of microstructural techniques for work hardening increase after SPD. Since the uniform strain of the **An** material is $\varepsilon_u \approx 0.21$, it is concluded that for the same total deformation ($\varepsilon \approx 2.1$), **An+ECAP+MAC** led to a uniform strain $\approx$ 20% of that for the **An** material. On the other hand, a softening of about 30 MPa resulted from the MAC after the ECAP, as indicated in Figure 2.2, corresponding to a loss of $\approx$ 23% of the post-ECAP strength of the material ($\approx$ 130 MPa).

2.5 Conclusions

Low strain amplitude Multi Axial Compression (MAC) in Aluminum previously submitted to ECAP softens the material and increases its subsequent monotonic work hardening rate, without changes in the dimensions of the material and thus leading to the recovery of a substantial part of its pre-ECAP uniform strain under tension. An increase in the number of MAC cycles, as well as a decrease in the strain amplitude per cycle, cause increasing softening levels and gains in the work hardening capacity and tensile uniform strain (ε_u) of the material. Adequate number of cycles and cyclic strain amplitudes should be experimentally selected for each desired set of final mechanical properties.

2.6 Acknowledgments

The authors are grateful for the financial support of the Brazilian Education Ministry, through the CAPES/PROEX and PROF programs of the Post Graduate Programs in Metallurgical and Materials Engineering and in Mechanical Engineering at UFMG, respectively, as well as the support of MCTI/CNPq and of FAPEMIG. The authors are thankful to F. Bubani for help in the mathematical analysis of the present stress-strain curves.

2.7 References

[1] ASM Handbook. Properties and selection: Nonferrous alloys and special-purpose materials. 10th ed. Ohio: American Society for Metals - ASM International, v. 2, 1990.

[2] I. Sabirov, M.Y. Murashkin, R.Z. Valiev, Nanostructured aluminium alloys produced by severe plastic deformation: New horizons in development, Mater. Sci. Eng. A, 560 (2013), pp. 1-24.

[3] R.Z. Valiev, T.G. Langdon, Principles of equal-channel angular pressing as a processing tool for grain refinement, Prog. Mater. Sci., 51 (2006), pp. 881-981.

[4] Y. Saito, N. Tsuji, H. Utsunomiya, T. Sakai, R.G. Hong, Ultra-fine grained bulk aluminum produced by accumulative roll-bonding (ARB) process, Scripta Mater., 39 (1998), pp. 1221-1227.

[5] A.P. Zhilyaev, T.G. Langdon, Using high-pressure torsion for metal processing: Fundamentals and applications, Prog. Mater. Sci., 53 (2008), pp. 893-979.

[6] R.Z. Valiev, M.Y. Murashkin, A. Kilmametov, B. Straumal, N.Q. Chinh, T.G. Langdon, Unusual super-ductility at room temperature in an ultrafine-grained aluminum alloy, J. Mater. Sci., 45 (2010), pp. 4718-4724.

[7] T. Sakai, H. Miura, X. Yang, Ultrafine grain formation in face centered cubic metals during severe plastic deformation, Mater. Sci. Eng. A, 499 (2009), pp. 2-6.

[8] T. Sakai, A. Belyakov, R. Kaibyshev, H. Miura, J.J. Jonas, Dynamic and post-dynamic recrystallization under hot, cold and severe plastic deformation conditions, Prog. Mater. Sci., 60 (2014), pp. 130-207.

[9] Q.F. Zhu, L. LI, C.Y. Ban, Z.H. Zhao, Y.B. Zuo, J.Z. Cui, Structure uniformity and limits of grain refinement of high purity aluminum during multi-directional forging process at room temperature, Trans. Nonf. Met. Soc. of China, 24 (2014), pp. 1301-1306.

[10] X. Xu, Q. Zhang, N. Hu, Y. Huang, T.G. Langdon, Using an Al–Cu binary alloy to compare processing by multi-axial compression and high-pressure torsion, Mater. Sci. Eng. A, 588 (2013), pp. 280-287.

[11] Y.G. Jin, H.M. Baek, S.K. Hwang, Y.T. Im, B.C. Jeon, Continuous high strength aluminum bolt manufacturing by the spring-loaded ECAP system, J. Mater. Process. Technol., 212 (2012), pp. 848-855.

[12] K. Edalati, T. Furuta, T. Daio, S. Kuramoto, Z. Horita, High Strength and High Uniform Ductility in a Severely Deformed Iron Alloy by Lattice Softening and Multimodal-structure Formation, Mater. Res. Letters, 3 (2015), pp. 197-202.

[13] G.J. Fan, H. Choo, P.K. Liaw, E.J. Lavernia, Plastic deformation and fracture of ultrafine-grained Al–Mg alloys with a bimodal grain size distribution, Acta Mater., 54 (2006), pp. 1759-1766.

[14] B.Q. Han, J.Y. Huang, E.J. Zhu, E.J. Lavernia, Strain rate dependence of properties of cryomilled bimodal 5083 Al alloys, Acta Mater., 54 (2006), pp. 3015-3024.

[15] Y. Wang, M. Chen, F. Zhou, E. Ma, High tensile ductility in a nanostructured metal, Nature, 419 (2002), pp. 912-915.

[16] S. Cheng, Y.T. Zhao, E. Zhu, Optimizing the strength and ductility of fine structured 2024 Al alloy by nano-precipitation, Acta Mater., 55 (2007), pp. 5822-5832.

[17] M. Hockauf, L.W. Meyer, B. Zillman, M. Hietschold, S. Schultze, L. Krueger, Simultaneous improvement of strength and ductility of Al–Mg–Si alloys by combining equal-channel angular extrusion with subsequent high-temperature short-time aging, Mater. Sci. Eng. A, 503 (2009), pp. 167-171.

[18] P.E. Armstrong, J.E. Hockett, O.D. Sherby, Large strain multidirectional deformation of 1100 aluminum at 300 K, J. Mech. Phys. Solids, 30 (1982), pp. 37-58.

[19] R.Z. Valiev, R.K. Islamgaliev, I.V. Alexandrov, Bulk nanostructured materials from severe plastic deformation, Prog. Mater. Sci., 45 (2000), pp. 103-189.

[20] Y. Iwahashi, Z. Horita, M. Nemoto, T.G. Langdon, Principle of equal-channel angular pressing for the processing of ultra-fine grained materials, Scripta Mater., 35 (1996), pp. 143-146.

[21] I.J. Beyerlein, D.J. Alexander, C.N. Tomé, Plastic anisotropy in aluminum and copper pre-strained by equal channel angular extrusion, J. Mater. Sci., 42 (2007), pp. 1733-1750.

[22] E.A. El-Danaf, M.S. Soliman, A.A. Almajid, M.M. El-Rayes, Enhancement of mechanical properties and grain size refinement of commercial purity aluminum 1050 processed by ECAP, Mater. Sci. and Eng. A, 458 (2007), pp. 226-234.

[23] A. Kundu, R. Kapoor, R. Tewari, J.K. Chakravartty, Severe plastic deformation of copper using multiple compression in a channel die, Scripta Mater., 58 (2008), pp. 235-238.

[24] T. Lee, K. Park, D.J. Lee, J. Jeong, S.H. Oh, H.S. Kim, C.H. Park, C.S. Lee, Microstructural evolution and strain-hardening behavior of multi-pass caliber-rolled Ti–13Nb–13Zr, Mater. Sci Eng A, 648 (2015), pp. 359-366.

3. Artigo 2

3.1 Title e Abstract

Microstructural evolution in the low strain amplitude multi-axial compression (LSA-MAC) after equal channel angular pressing (ECAP) of aluminum

Low strain amplitude multi-axial compression (LSA-MAC) increases the work hardening capacity and uniform ductility of Aluminum after Severe Plastic Deformation (SPD) through Equal Channel Angular Pressing (ECAP). The mechanisms associated with this processing after ECAP are analyzed. LSA-MAC after 1 ECAP pass in Aluminum softens the material and is connected to the stabilization of the dislocation structures induced by ECAP into a configuration displaying an increased fraction of High Angle Grain Boundaries (HAGB). This occurs for a lower total imposed strain than that through a sequence of high strain ECAP passes or high strain amplitude multi-axial compression (HAS-MAC).

Keywords: Metals and alloys; Equal Channel Angular Pressing (ECAP); Low Strain Amplitude Multi-Axial Compression (LSA-MAC), Severe Plastic Deformation (SPD); Work hardening; Microstructures.

3.2 Introduction

The production of ultra-fine grained (UFG), high strength metals, through Severe Plastic Deformation (SPD) usually employs Equal Channel Angular Pressing (ECAP), High Pressure Torsion (HPT) or High Strain Amplitude ($\Delta\varepsilon$) Multi-Axial Compression (HSA-MAC, $\Delta\varepsilon \approx 0.5$ to 0.8) [1], also widely known as Multi-Directional Forging (MDF) [2]. UFG materials exhibit low or negative work hardening rate and a low tensile uniform elongation after processing. Microstructural changes in the material before SPD have been developed for increasing their post-SPD low work hardening capacity [3]. A recent study by the present authors [4] showed that Low Strain Amplitude Multi-Axial Compression (LSA-MAC, $\Delta\varepsilon = 0.075$) after ECAP led to an increase in the work hardening capacity of aluminum; this is simpler than pre-SPD microstructural manipulations and can be used for all materials. The present objective is to analyze the

microstructural aspects connected to this new procedure. The results indicate that the effects of LSA-MAC after ECAP are associated with the stabilization of the dislocation structures after a much lower total strain than that observed in the usual SPD techniques.

3.3 Experimental

As-cast 1070 Aluminum specimens underwent: 1 ECAP pass, annealing, another ECAP pass, LSA-MAC (12 compressions, $\Delta\varepsilon = 0.075$) and simple compression. Detailed experimental procedures have been described elsewhere [4]. The material was evaluated in the following conditions: (i) as-cast, 1 ECAP pass and annealed (**An**) (ii) annealed and 1 ECAP pass (**An+ECAP**) (iii) annealed, 1 ECAP pass and LSA-MAC (**An+ECAP+LSA-MAC**) (iv) annealed, 1 ECAP pass, LSA-MAC and compression (**An+ECAP+LSA-MAC+COMP).** The analyses involved microhardness testing, Electron Backscattered Diffraction (EBSD) and Transmission Electron Microscopy (TEM) in the specimen cross-section orthogonal to (i) the extrusion direction for **An** and **An+ECAP**, (ii) the first compressed direction for the **An+ECAP+LSA-MAC** and (iii) the compression direction for the **An+ECAP+LSA-MAC+COMP**. Vickers microhardness employed a Mitutoyo MVK-H1 with a 500g load for 15s; surface preparation involved initial 600 mesh paper, electrolytic polishing (700 ml C_2H_5OH, 120ml distilled H_2O, 100ml $C_4H_9OC_2H_4OH$, 68ml 70% $HClO_4$ at 35V for 45s and a stainless steel cathode). 20 measurements were taken at evenly distributed points in the specimen section. EBSD and TEM were performed in the central part of the above mentioned cross-sections. At least 3 different areas were analyzed for each processing condition; since no remarkable differences were observed for these different areas, one of them was chosen as a typical one for the present paper. TEM employed a Tecnai G2-20 SuperTwin FEI-200kV (UFMG) and a Philips CM200 Ultratwin–200kV (Bariloche); specimens were ground to a thickness of 100μm, punched into 3mm diameter discs and perforated with a double jet TENUPOL 5 using a 30% nitric acid–methanol solution at 243K. EBSD specimens were prepared similarly to those for microhardness. A Quanta FEG 3D FEI SEM with a Bruker QUANTAX EBSD analysis system was utilized. Data were processed with the Bruker Esprit 2 software. Detection of neighboring grains was

set at a disorientation angle of 2º. For the large grained **An** specimen the area was 30820μm^2 and step size 270nm; for the other conditions, the area was 4802μm^2 and step size 62nm. ~ 98.5% and ~ 90% of the points were indexed for the **An** specimen and for the other specimens, respectively. Noise elimination completed the absent indexing for some points, through an averaging from neighboring points.

3.4 Results and discussion

The average microhardness for the various conditions were **An**: 21.2 ± 1.7HV, **An+ECAP**: 45.3 ± 2.9HV, **An+ECAP+LSA-MAC**: 36.5 ± 1.8HV, **An+ECAP+LSA-MAC+COMP**: 40.9 ± 2.0HV. LSA-MAC after the ECAP softens the material, whereas the final compression step hardens it again, in line with a previous report [4].

Figure 3.1 displays the Orientation Imaging Microscopy (OIM) results for the conditions: (a) **An**, (b) **An+ECAP**, (c) **An+ECAP+LSA-MAC** and (d) **An+ECAP+LSA-MAC+COMP.** The **An** grains (Figure 3.1a) are approximately equiaxed and single colored. The **An+ECAP** condition (Figure 3.1b) exhibits large and small elongated grains; the former correspond to the original **An** grains and display color hues, connected to regions with small disorientations, indicating the presence of dislocation cells/subgrains. The additional strain imposed by LSA-MAC after ECAP increases the fraction of areas with small elongated grains (Figure 3.1c), often fragmented along their lengths. LSA-MAC caused a fast evolution of initial grains towards equiaxed UFGs due to the variation in the shearing planes associated with the changes in the compression direction [5], similarly to the Bc route in ECAP [6]. The microstructure for the **An+ECAP+LSA-MAC+COMP** condition (Figure 3.1d) displays color hues, similarly to the situation after ECAP, indicating the presence of cell/subgrains.

Figure 3.2 displays the grain boundary characteristics and disorientation distributions for the conditions, respectively: (3.2a, 3.2b) **An**, (3.2c, 3.2d) **An+ECAP**, (3.2e, 3.2f) **An+ECAP+LSA-MAC** and (3.2g, 3.2h) **An+ECAP+LSA-MAC+COMP**. Comparing Figures 3.2a, 3.2b with Figures 3.2c, 3.2d indicates that ECAP refined the grains, displaying a predominance of grain disorientations in the range of 2º to 5º (0.637). ECAP

also leads to a fraction of 0.866 LAGB (disorientaton angles < 15º), similarly to reports in the literature [7, 8]. Figures 3.2e, 3.2f show that LSA-MAC decreased the fraction of grain boundaries with disorientations in the range of 2º – 5º (0.637 after ECAP, 0.496 after LSA-MAC), coupled to an increase in the fraction of HAGBs (grain disorientation > 15º) from 0.134 after ECAP to 0.251 after LSA-MAC. Compression after ECAP+LSA-MAC is connected to a grain disorientation distribution similar to that after ECAP (Figures 3.2g, 3.2h, HAGB fraction of 0.123), reverting the tendency of increased HAGB fraction caused by LSA-MAC.

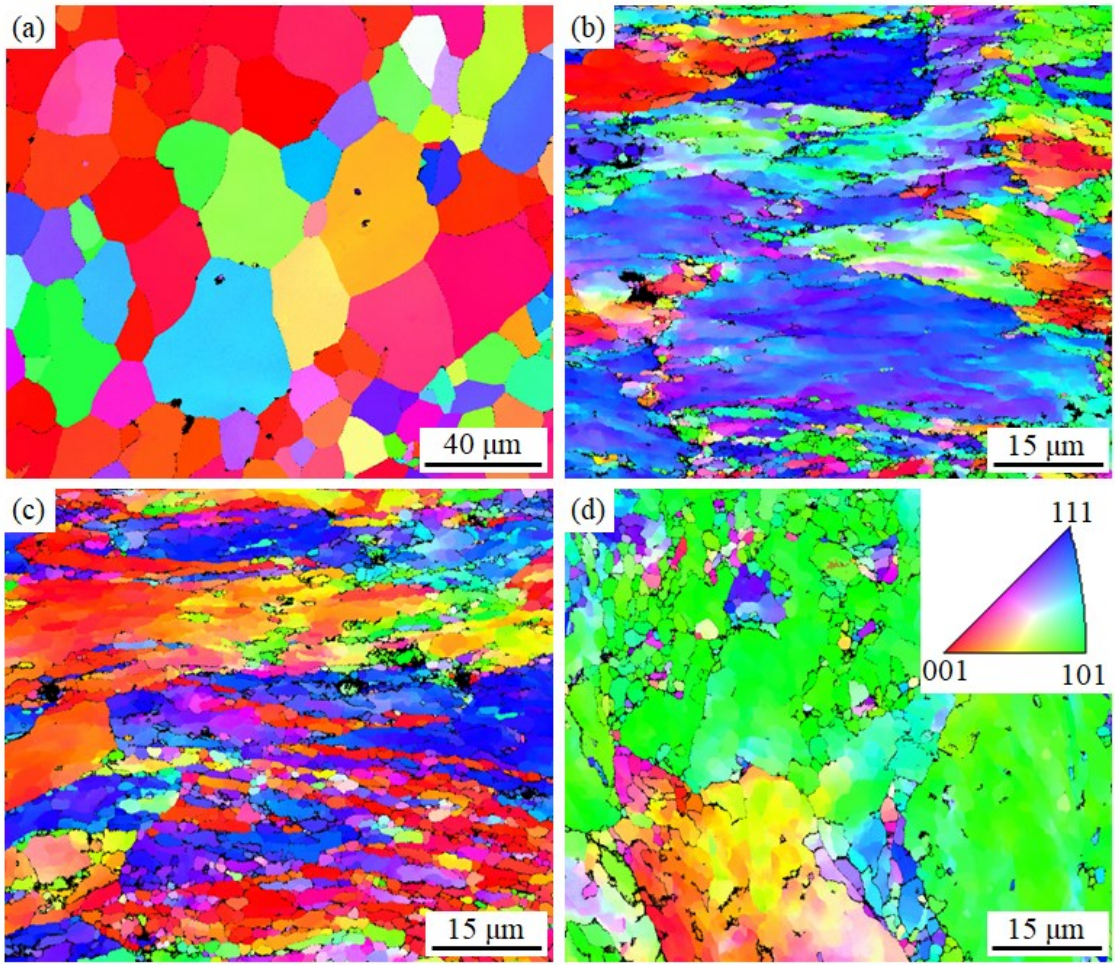

Figure 3.1 – OIM images for specimens in the conditions: (a) **An**, (b) **An+ECAP**, (c) **An+ECAP+LSA-MAC** and (d) **An+ECAP+LSA-MAC+COMP**.

Figure 3.3 displays TEM images for the conditions: (3.3a, 3.3b) **An+ECAP**, (3.3c, 3.3d) **An+ECAP+LSA-MAC** and (3.3e, 3.3f) **An+ECAP+LSA-MAC+COMP**. **An+ECAP**

material displays elongated and equiaxed grains with internal dislocations (Figures 3.3a, 3.3b), similarly to the literature [6]. The grains for the **An+ECAP+LSA-MAC** condition (Figures 3.3c, 3.3d) are more equiaxed and somewhat smaller than those after **An+ECAP**; displaying intragranular dislocation structures (see the lower right corner, Figure 3.3c). Compression after LSA-MAC (**An+ECAP+LSA-MAC+COMP**, Figures 3.3e, 3.3f) lead to grain sizes somewhat larger than for **An+ECAP+LSA-MAC** (Figures 3.3c, 3.3d), but without any remarkable differences.

SPD initially forms dislocation tangles and cell walls; that thin and evolve into more stable and lower energy dislocation configurations such as HAGBs [9] as strain rises. This is observed in Aluminum after 4 ECAP passes [10] and after 6 high strain amplitude Multi-axial compression (HSA-MAC) cycles with strain amplitude $\Delta\varepsilon = 0.80$ [11]. The strength of Copper decreases after more than 4 ECAP passes stabilizes up to 16 ECAP passes [12]. This is also reported for the compression in the transversal direction of copper after ECAP and Aluminum after 2 ECAP passes [10]. Softening also occurs in copper [13] and aluminum [11] in plane strain HSA-MAC after strains $\approx 4 - 5$, both for a strain amplitude $\Delta\varepsilon = 0.8$. Data for copper show that, as the number of ECAP passes is raised up to 16, grain size decreases up to 1 – 2 ECAP passes, followed by grain size stabilization; HAGB/unit area increases up to about 12 passes and slowly decreases up to the 16th pass. Dislocation density rises up to the 4th pass and slowly decreases and stabilizes up to the 16th pass [14].

The present results show that a straining of 1.15 by ECAP followed by LSA-MAC with a total strain of 0.9 (12 steps, $\Delta\varepsilon = 0.075$), totaling a strain of 2.05, led to an HAGB fraction of 0.251, similarly to that for an ECAP strain of ~3 in Al 99,99% [7] and ~4 in Al 1%Mg [8], and to a strain ~4.6 in the HSA-MAC of Aluminum [11] and to a decrease in the material hardness. ECAP+LSA-MAC causes effects similar to those described above for Copper [13, 14] and Aluminum [11], for a much lower total strain than those reported in the literature. The monotonic compression after ECAP+LSA-MAC interrupted the increase in the HAGB fraction caused by LSA-MAC after ECAP and reversed the evolution of this fraction.

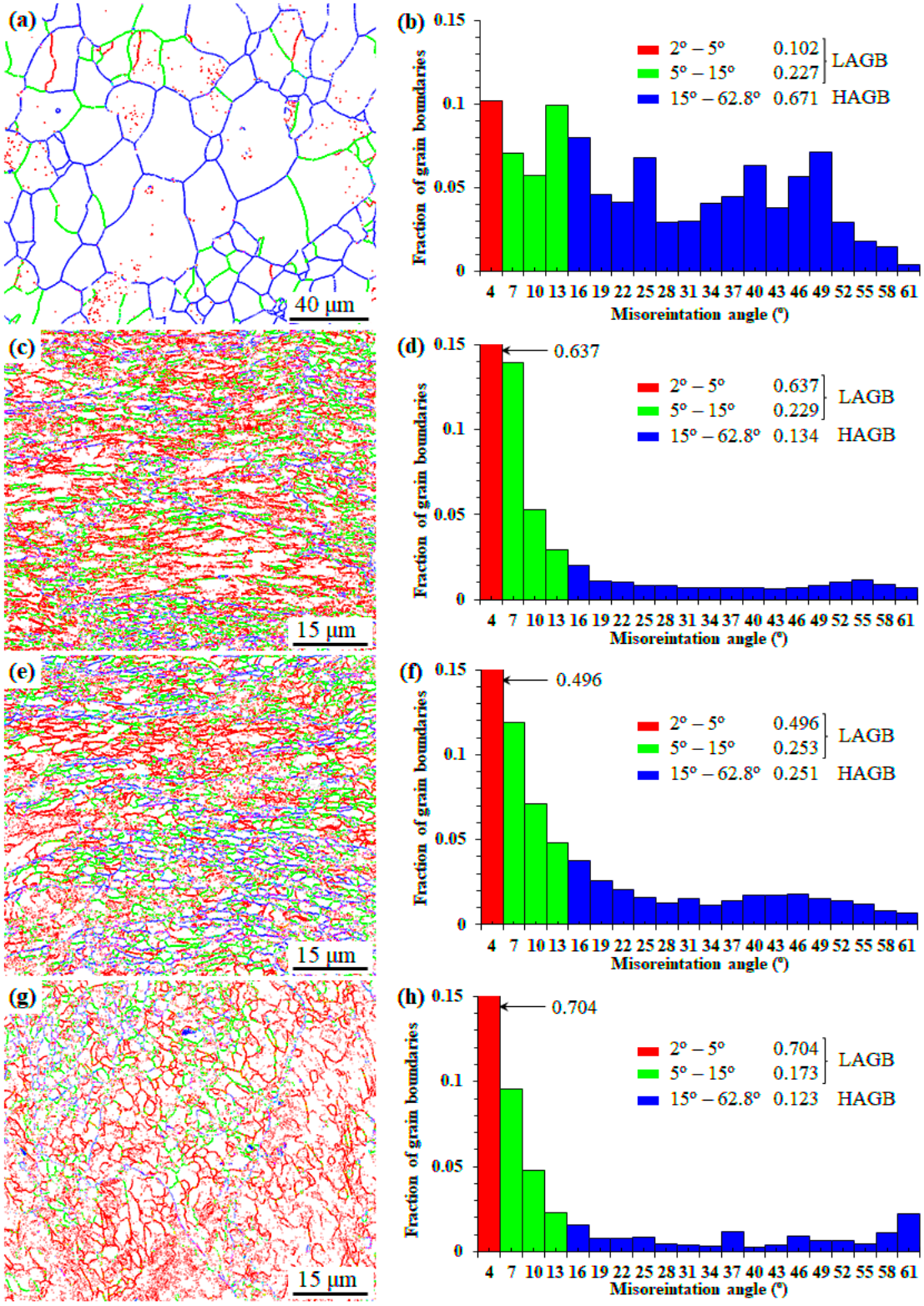

Figure 3.2 – Grain boundary characteristics and grain disorientation distributions for specimens: (a, b) **An**, (c, d) **An+ECAP**, (e, f) **An+ECAP+LSA-MAC** and (g, h) **An+ECAP+LSA-MAC+COMP**.

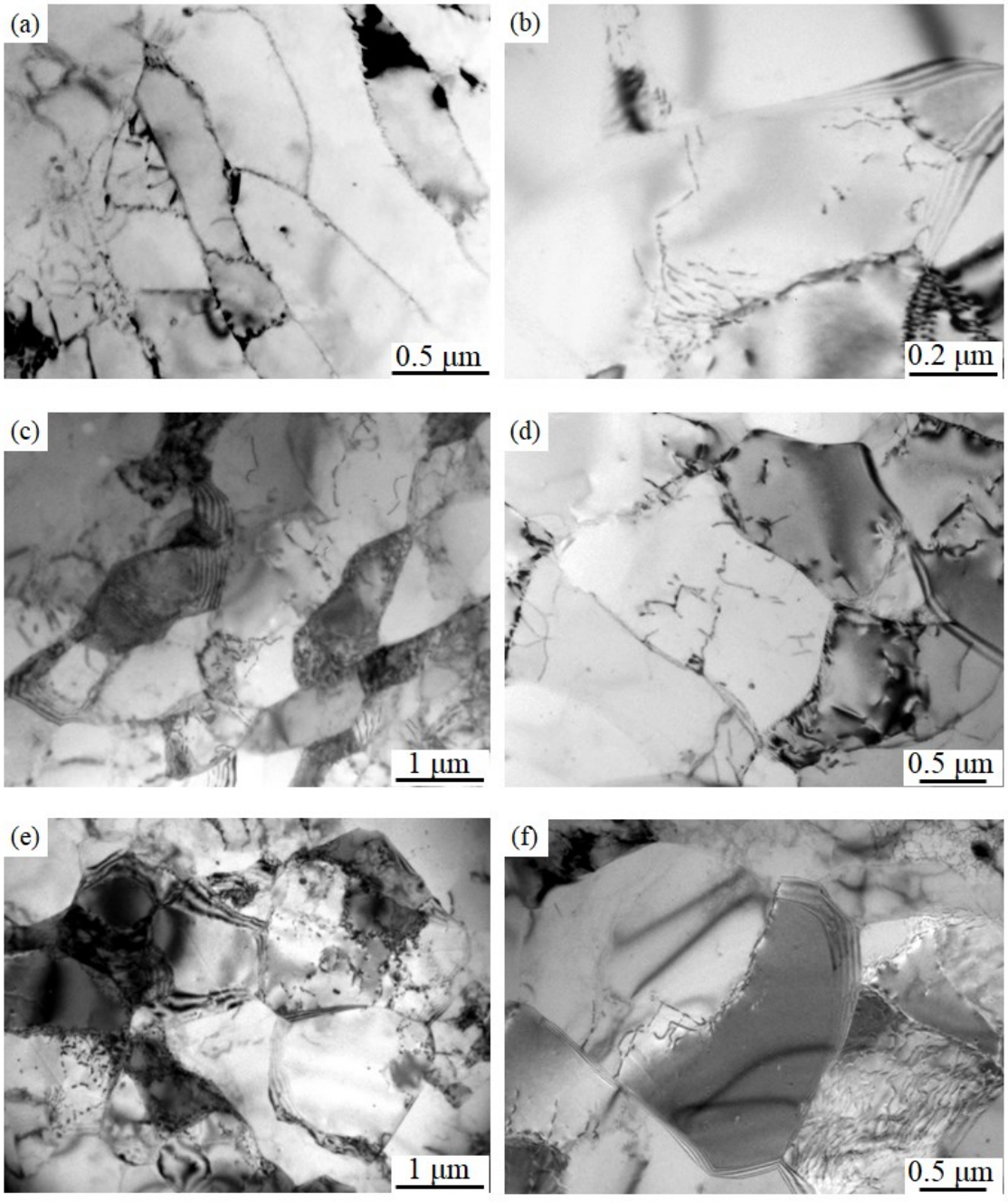

Figure 3.3 – TEM images for the following conditions: (a, b) **An+ECAP**, (c, d) **An+ECAP+LSA-MAC** and (e, f) **An+ECAP+LSA-MAC+COMP**.

3.5 Conclusions

SPD through ECAP and high strain amplitude multi-axial compression (HSA-MAC, $\Delta\varepsilon \approx 0.5$ to 0.8) stabilizes the dislocation structures after a large total strain and number of deformation steps.

Low strain amplitude Multi-axial compression (LSA-MAC, $\Delta\varepsilon = 0.075$) after ECAP accelerates, in terms of a lowered total imposed strain, the stabilization of the dislocation structures into lower energy arrangements, leading to softening and increased work hardening capacity of the material for further monotonic straining.

3.6 Acknowledgments

The authors are grateful for the financial support of the Brazilian Education Ministry, through the CAPES/PROEX and PROF programs of the Graduate Program in Metallurgical and Materials Engineering at UFMG and of MCTI/CNPq and FAPEMIG.

3.7 References

[1] R.Z. Valiev, R.K. Islamgaliev, I.V. Alexandrov, Bulk nanostructured materials from severe plastic deformation,Prog. Mater. Sci. 45 (2000) 103-189.

[2] Y. Estrin, A. Vinogradov, Extreme grain refinement by severe plastic deformation: A wealth of challenging science, Acta Mater. 61 (2013) 782–817.

[3] I. Sabirov, M.Y. Murashkin, R.Z. Valiev, Nanostructured aluminium alloys produced by severe plastic deformation: New horizons in development,Mater. Sci. Eng. A 560 (2013) 1-24.

[4] C.G. Faria, N.G.S. Almeida, M.T.P. Aguilar, P.R. Cetlin, Increasing the work hardening capacity of equal channel angular pressed (ECAPed) aluminum through multi-axial compression (MAC),Mater. Lett. 174 (2016) 153-156.

[5] T. Sakai, H. Miura, X. Yang, Ultrafine grain formation in face centered cubic metals during severe plastic deformation, Mater. Sci. Eng. A 499 (2009) 2-6.

[6] T.G. Langdon, The principles of grain refinement in equal-channel angular pressing, Mater. Sci. Eng. A 46 (2007) 3-11.

[7] M. Kawasaki, Z. Horita, T.G. Langdon, Microstructural evolution in high purity aluminum processed by ECAP, Mater. Sci. Eng. 524 (2009) 143-150.

[8] C. Xu, Z. Horita, T.G. Langdon, Microstructural evolution in an aluminum solid solution alloy processed by ECAP, Mater. Sci. Eng. A 528 (2011) 6059-6065.

[9] R.Z. Valiev, Y.V. Ivanisenko, E.F. Rauch, B. Baudelet, Structure and deformaton behaviour of Armco iron subjected to severe plastic deformation, Acta Mater. 44 (1996) 4705-4712.

[10] I.J. Beyerlein, D.J. Alexander, C.N. Tomé, Plastic anisotropy in aluminum and copper pre-strained by equal channel angular extrusion, J. Mater. Sci. 42 (2007) 1733-1750.

[11] R. Kapoor, A. Sarkar, R. Yogi, S.K. Shekhawat, I. Samajdar, J.K. Chakravartty, Softening of Al during multi-axial forging in a channel die, Mater. Sci. Eng. A 560 (2013) 404-412.

[12] F. Dalla Torre, R. Lapovok, J. Sandlin, P.F. Thomson, C.H.J. Davies, E.V. Pereloma, Microstructures and properties of copper processed by equal channel angular extrusion for 1–16 passes, Acta Mater. 52 (2004) 4819-4832.

[13] A. Kundu, R. Kapoor, R. Tewari, J.K. Chakravartty, Severe plastic deformation of copper using multiple compression in a channel die, Scr. Mater. 58 (2008) 235-238.

[14] H.J. Maier, P. Gabor, N. Gupta, I. Karaman, M. Haouaoui, Cyclic stress-strain response of ultrafine grained copper, Int. J. Fatigue 28 (2006) 243–250.

4. CONCLUSÕES

A compressão uniaxial do material submetido a um passe de ECAP segundo à direção X, situação que promoveria a reversão do escorregamento no plano de cisalhamento ativado pelo ECAP, apresenta um pico inicial e posterior amaciamento. Isto provavelmente ocorre pela ativação de planos de deslizamentos não ativados previamente pelo passe de ECAP.

A distorção das faces laterais causa irregularidades nas partes iniciais das sucessivas curvas tensão x deformação no processamento multiaxial devido ao abaulamento e à falta de paralelismo entre as faces perpendiculares à direção de processamento após o primeiro passe.

A compressão multiaxial com baixa amplitude de deformação em alumínio pré-encruado por um passe de ECAP amacia o material e reestabelece parte da ductilidade perdida pelo primeiro processamento, um passe de ECAP.

A compressão multiaxial com baixa amplitude e deformação após um passe de ECAP estabiliza a estrutura de deslocações em um arranjo de menor energia, levando ao amaciamento e à recuperação de parte da capacidade de encruamento para posterior compressão uniaxial de forma mais rápida que ocorre para ECAP ou MAC separadamente.

5. SUGESTÕES PARA TRABALHOS FUTUROS

Realizar a compressão multiaxial dentro de uma matriz que restrinja as expansões laterais das amostras, inibindo assim a ocorrência do abaulamento.

Realizar os ensaios de compressão multiaxial apenas em duas direções, de forma a aproximar os estudos às técnicas de conformações mecânicas industriais.

Estudar o processamento multiaxial para amostras processadas por dois e quatro passes de ECAP, de forma a se avaliar as diferentes microestruturas desenvolvidas por deformação severa submetidas à compressão multiaxial.

Realizar a mesma técnica utilizando outros materiais e ligas para verificar a ocorrência ou não dos fenômenos observados para o alumínio puro.

6. ANEXOS

São anexados a esta tese os dois artigos conforme publicados.

Materials Letters 174 (2016) 153–156

Contents lists available at ScienceDirect

Materials Letters

journal homepage: www.elsevier.com/locate/matlet

Increasing the work hardening capacity of equal channel angular pressed (ECAPed) aluminum through multi-axial compression (MAC)

Cleber Granato de Faria [a], Natanael Geraldo Silva Almeida [b], Maria Teresa Paulino Aguilar [c], Paulo Roberto Cetlin [d,*]

[a] Post-graduate Program in Metallurgical, Materials and Mining Engineering, Brazil
[b] Post-graduate Program in Mechanical Engineering, Brazil
[c] Dept of Construction and Materials, Brazil
[d] Dept of Mechanical Engineering, Brazil

ARTICLE INFO

Article history:
Received 18 January 2016
Received in revised form
3 March 2016
Accepted 19 March 2016
Available online 21 March 2016

Keywords:
Equal Channel Angular Pressing (ECAP)
Multiaxial compression (MAC)
Work hardening

ABSTRACT

The low strength of commercial purity aluminum can be increased by solid solution, precipitation/aging, work hardening and grain size decrease. The latter has been extensively studied utilizing Severe Plastic Deformation (SPD), leading, however, to a negligible final uniform tensile ductility of the material due to its low or negative work hardening rates. Microstructural and compositional techniques have been used to partially circumvent this problem. Multi-axial compression (MAC) of previously compressed aluminum can soften the material and lead to increased work hardening capacity under ulterior monotonic compression. In the present research, MAC was applied to aluminum after SPD employing Equal Channel Angular Pressing (ECAP). The material softened after MAC, and its ulterior compression evolved with a much higher work hardening rate than in the absence of MAC, thus opening a new possibility of mechanically increasing the work hardening capacity and uniform ductility of aluminum (and other materials) after ECAP.

1. Introduction

Aluminum is widely available and presents, low cost, light weight, corrosion resistance, ductility and attractive finish. High purity aluminum displays however a yield strength of only about 10 MPa [1], which can be increased through solid solution, precipitation/aging, work hardening and grain refinement. The latter has led to many researches in order to obtain exceptionally small grain sizes (below 1 μm) through Severe Plastic Deformation (SPD) processes [2].

SPD has been achieved through ECAP (Equal Channel Angular Pressing) [3], ARB (Accumulative Roll Bonding) [4], HPT (High Pressure Torsion) [5], and MAC (Multi Axial Compression, also known as Multi Axial Forging - MDF) [6–10]. ECAP is attractive because it can produce large samples and is adaptable to continuous and high output processes [11], leading to end products useful for structural purposes.

The material uniform ductility after SPD is very limited in the low temperature regime, for stress states with tensile components such as sheet forming, bending and simple tension [12]. This is caused by the negligible or negative work hardening rates observed in the monotonic deformation of materials after SPD [2]. Some techniques have been suggested in order to alleviate this problem: (i) a bi-modal grain size distribution [13–15] (ii) the introduction of nano-precipitates in the material [16,17] and (iii) high Zn contents in aluminum [6]. These approaches involve complex microstructural and compositional aspects.

An early study connected to MAC in aluminum was performed by Armstrong et al. [18], involving strain amplitudes from 0.075 to 0.33 at room temperature and comparing the results with those for monotonic compression. This contrasts to more recent analyses, [7–9,19] where strain amplitudes range from 0.4 to 0.6, homologous temperatures vary from 0.1 to 0.5 and there is no comparison with monotonic compressions. Armstrong et al. [18] report that MAC led to: (a) lower work hardening and strength than monotonic compression, (b) lower work hardening as the strain amplitude decreased, (c) softening of monotonically compressed material when submitted to a subsequent MAC, provided that the strain amplitude in MAC were lower than the initial monotonic strain and (d) if the material thus softened underwent a monotonic compression again, it would work harden at a higher

* Correspondence to: Universidade Federal de Minas Gerais, Escola de Engenharia, Bloco I, Av. Antonio Carlos 6627, Pampulha, CEP 31270-901, Minas Gerais, Brazil.
E-mail addresses: clebergranato@gmail.com (C.G. de Faria), natanaelgsa@gmail.com (N.G. Silva Almeida), teresa@demc.ufmg.br (M.T. Paulino Aguilar), pcetlin@demec.ufmg.br (P.R. Cetlin).

http://dx.doi.org/10.1016/j.matlet.2016.03.112
0167-577X/

rate than for full previous monotonic compression, for the same levels of deformation.

The above findings suggest that the post-SPD work hardening capacity and consequent uniform tensile ductility of materials would increase through the application of MAC with a strain amplitude lower than the applied monotonic SPD deformation, but that some strength loss is also expected. This approach is simpler than the microstructural and compositional aspects already mentioned [6,13–17] utilized in order to increase the post-SPD ductility of the material. It should be remembered that MAC does not change the dimensions of the initial material, and thus the work hardening increase can be viewed as available in the pre-MAC treated material.

The present paper presents experimental results concerning the strength and work hardening behavior of commercial purity aluminum under monotonic compression after one ECAP pass followed by a limited number of low strain amplitude MAC. As predicted, the material softened after MAC and displayed high work hardening rates in the final monotonic compression step. No similar investigation was found in the literature.

2. Experimental

The material was commercial purity cast aluminum (Al-99.77, Fe-0.15, Si-0.06 wt%) in cylinders 150 mm in diameter. Samples $15.8 \times 15.8 \times 100$ mm³ were machined from this bar, with the long dimension parallel to the cylinder axis. These were deformed and annealed (hereafter referred to as **An** material) in order to break the as-cast initial structure; deformation involved one ECAP pass with channels at a 90° angle and sections of 15.9×15.9 mm^2, imposing a strain of $\varepsilon \approx 1.15$ [20], at room temperature and at ≈ 20 mm/min; the die/specimen interface was lubricated with molybdenum disulfide. The processed samples were annealed at 623 K for 7200 s.

Monotonic compression and tension tests were performed in the **An** material, utilizing compression specimens with cross-section of 16.5×16.5 mm^2 and a height of 28.0 mm (height/width = 1.7) and tension specimens 35 mm long and 5.0 mm in diameter, both lying along the X direction in Fig. 1a, which was also the compression and tension direction. The compression die/specimen interfaces were lubricated with molybdenum disulfide paste, and testing was interrupted for every $\varepsilon \approx 0.1$ increment for interface re-lubrication, up to a total axial strain of $\varepsilon \approx 2.0$. Following Armstrong's [18] recommendations, specimens were re-machined back to the initial height/width ratio of 1.7 after deformations of $\varepsilon \approx 0.7$, in order to avoid excessive specimen distortions.

The annealed material ("**An**" material) was submitted to another ECAP pass ("**An+ECAP**" material) identical to the above described one, and performed along the "X" direction in Fig. 1a. MAC was performed in the **An+ECAP** material ("**An+ECAP+MAC**" material). The specimens had the dimensions: 13.00 (direction X), 12.06 (direction Y) and 12.52 (direction Z) mm³, with a strain amplitude $\varepsilon \approx 0.075$. The interface between the compression die and the specimen was lubricated with molybdenum disulfide. Compressions sequence followed the X, Z and Y directions (Fig. 1b). For all compression steps in an isotropic material deforming homogeneously, the direction under compression had (i) an initial length of 13.00 mm after the previous $\varepsilon \approx 0.075$ straining in an orthogonal direction, and (ii) underwent a decrease in length of 0.94 mm. MAC was performed for 4 cycles (a total of 12 compressions), totaling an external strain of $\varepsilon \approx 0.9$. According to Armstrong [18] this leads to approximately 50% of the total possible softening through MAC in the **An+ECAP** material, considered as a reasonable goal in terms of final uniform ductility without an excessive loss of strength of the material.

An+ECAP+MAC specimens were submitted to monotonic compression along the X axis, in order to evaluate its post-MAC work hardening and strength.

All testing was performed in duplicate in an INSTRON 5582 universal testing machine, at a crosshead speed of 0005 mm/s. No remarkable differences were observed when comparing the results obtained for both sets of specimens.

3. Results and discussion

Fig. 2 displays the stress-strain curves in monotonic compression for the **An**, **An+ECAP** and **An+ECAP+MAC** materials along direction X, as well as in the MAC for the **An+ECAP** material.

The stress-strain curve in the first compression of the **An+ECAP** material (along direction X) displays an initial peak ("spike") above the monotonic compression curve, followed by negative work hardening, similarly to the "cross-test effects" reported by Beyerlein et al. [21] for 99.99 wt%Al. This is surprising, since the present post-ECAP compression in the X direction corresponds to a situation where slip in the shearing plane in ECAP is reversed on further compression, and should lead to Beyerlein's "reversed test effects" and no initial spike. El-Danaf's [22] results for 1050 aluminum also displayed a "spike effect" but lower in relation to the present one. It is suggested that simple compression after ECAP,

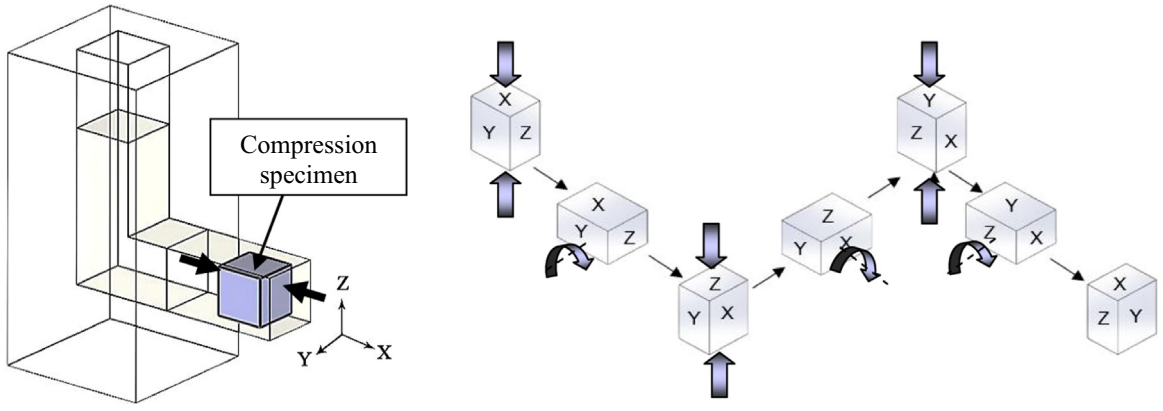

Fig. 1. – ECAP and compression testing in the present paper: (a) coordinate axes and direction of monotonic compression and (b) sequence of compressions in MAC processing.

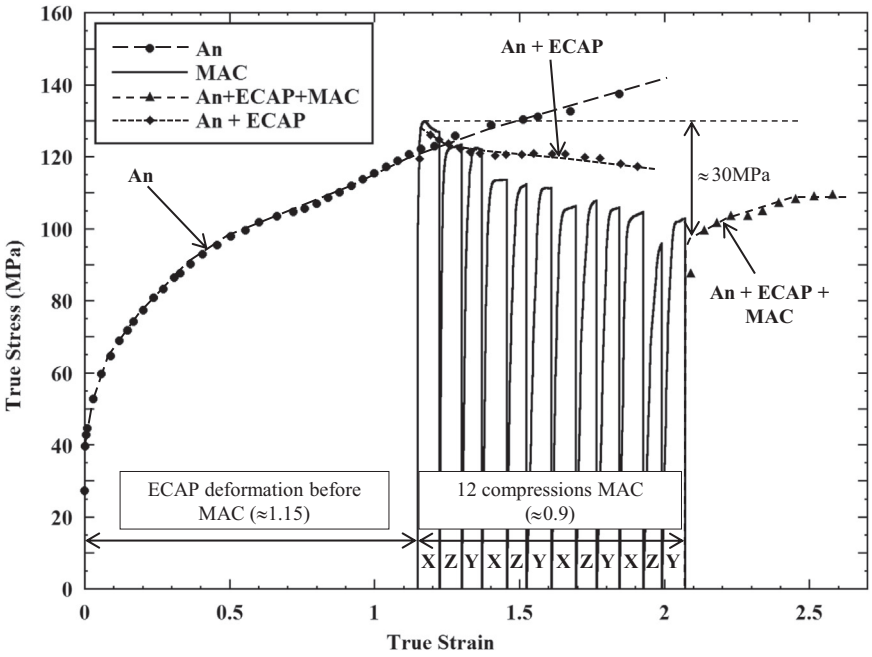

Fig. 2. – Stress – strain curves for the monotonic compression of the **An**, **An**+**ECAP** and **An**+**ECAP**+**MAC** materials, and for MAC in the ECAPed material.

along the present "X" direction, can also lead to the activation of slip systems not previously activated during ECAP, similarly to the situation in "cross-test-effects" [21].

The observation of the stress-strain curves displayed in Fig. 2 for the individual deformation steps during MAC indicates small variations in strain amplitude of the various steps, as well as situations where the initial parts of the curves display low levels of stress (see, e. g., the curve in the "Z" direction of the last MAC cycle). These phenomena are connected to lateral bulging of the samples in the previous deformation step. As the specimen is rotated and compressed, the initial part of the stress-strain curve corresponds to the "flattening" of the specimen surface by the compression platen. This also causes small errors in the average strain in the deformation step, since compression actually begins when the top of the specimen bulge contacts the compression platen. Similar bulging and consequent strain heterogeneity problems during MAC have been recently reported [9]. Armstrong et al. [18] also mention bulging problems, but state that specimen re-machining was necessary only after a total strain of 0.7 was reached. The use of dies in constrained MAC practically eliminates bulging problems [23], and thus seems to be a more convenient method for MAC than the current free compression.

Fig. 2 indicates that MAC caused a higher softening in the **An**+**ECAP** material than the monotonic compression along the X axis. The work hardening in the monotonic compression of the **An**+**ECAP**+**MAC** material is positive and obviously higher than the negative work hardening for the **An**+**ECAP** material, extrapolated to the straining interval of ≈ 2.1 to ≈ 2.6. Since MAC does not change the dimensions of the ECAPed material, the situation can be viewed as a direct increase in the work hardening capacity of the **An**+**ECAP** material.

Necking (and thus the uniform strain ε_u) in tensile testing occurs when $\theta=(d\sigma/d\varepsilon)/\sigma=1$ [24]. The variation of θ with strain was evaluated for the monotonic compression and tension of the **An** material and for the **An**+**ECAP**+**MAC** materials. For compression and tension, $\theta=1$ for $\varepsilon_u \approx 0.21$ to ≈ 0.23; all compressive strains above this strain range lead to immediate necking and to very low uniform strains under further tensile testing. This is the post-ECAP situation (strain of ≈ 1.15), where θ for monotonic compression becomes negative for very small strains (see the compression curve for the **An**+**ECAP** material). The same analysis for the **An**+**ECAP**+**MAC** material indicated that the $\theta=1$ condition is reached for $\varepsilon_u \approx 0.043$, which is higher than that reported for Ti-13Nb-13Zr [24] as a consequence of the use of microstructural techniques for work hardening increase after SPD. Since the uniform strain of the **An** material is $\varepsilon_u \approx 0.21$, it is concluded that for the same total deformation ($\varepsilon \approx 2.1$), **An**+**ECAP**+**MAC** led to a uniform strain $\approx 20\%$ of that for the **An** material. On the other hand, a softening of about 30 MPa resulted from the MAC after the ECAP, as indicated in Fig. 2, corresponding to a loss of $\approx 23\%$ of the post-ECAP strength of the material (≈ 130 MPa).

4. Conclusions

Low strain amplitude Multi Axial Compression (MAC) in aluminum previously submitted to ECAP softens the material and increases its subsequent monotonic work hardening rate, without changes in the dimensions of the material and thus leading to the recovery of a substantial part of its pre-ECAP uniform strain under tension. An increase in the number of MAC cycles, as well as a decrease in the strain amplitude per cycle, cause increasing softening levels and gains in the work hardening capacity and tensile uniform strain (ε_u) of the material. Adequate number of cycles and cyclic strain amplitudes should be experimentally selected for each desired set of final mechanical properties.

Acknowledgments

The authors are grateful for the financial support of the Brazilian Education Ministry (Grant 301034/2013-3), through the CAPES/PROEX and PROF programs of the Post Graduate Programs in Metallurgical and Materials Engineering and in Mechanical Engineering at UFMG, respectively, as well as the support of MCTI/CNPq and of FAPEMIG. The authors are thankful to F. Bubani for help in the mathematical analysis of the present stress-strain curves.

References

[1] ASM Handbook, 10th ed.,Properties and Selection: Nonferrous Alloys and Special-Purpose Materials, 2, American Society for Metals – ASM International, Ohio, 1990.

[2] I. Sabirov, M.Y. Murashkin, R.Z. Valiev, Nanostructured aluminium alloys produced by severe plastic deformation: new horizons in development, Mater. Sci. Eng. A 560 (2013) 1–24.

[3] R.Z. Valiev, T.G. Langdon, Principles of equal-channel angular pressing as a processing tool for grain refinement, Prog. Mater. Sci. 51 (2006) 881–981.

[4] Y. Saito, N. Tsuji, H. Utsunomiya, T. Sakai, R.G. Hong, Ultra-fine grained bulk aluminum produced by accumulative roll-bonding (ARB) process, Scr. Mater. 39 (1998) 1221–1227.

[5] A.P. Zhilyaev, T.G. Langdon, Using high-pressure torsion for metal processing: fundamentals and applications, Prog. Mater. Sci. 53 (2008) 893–979.

[6] R.Z. Valiev, M.Y. Murashkin, A. Kilmametov, B. Straumal, N.Q. Chinh, T. G. Langdon, Unusual super-ductility at room temperature in an ultrafine-grained aluminum alloy, J. Mater. Sci. 45 (2010) 4718–4724.

[7] T. Sakai, H. Miura, X. Yang, Ultrafine grain formation in face centered cubic metals during severe plastic deformation, Mater. Sci. Eng. A 499 (2009) 2–6.

[8] T. Sakai, A. Belyakov, R. Kaibyshev, H. Miura, J.J. Jonas, Dynamic and post-dynamic recrystallization under hot, cold and severe plastic deformation conditions, Prog. Mater. Sci. 60 (2014) 130–207.

[9] Q.F. Zhu, L. LI, C.Y. Ban, Z.H. Zhao, Y.B. Zuo, J.Z. Cui, Structure uniformity and Limits of Grain Refinement of High purity Aluminum during Multi-Directional Forging process at Room Temperature, Trans. Nonferr. Met. Soc. China 24 (2014) 1301–1306.

[10] X. Xu, Q. Zhang, N. Hu, Y. Huang, T.G. Langdon, Using an Al–Cu binary alloy to compare processing by multi-axial compression and high-pressure torsion, Mater. Sci. Eng. A 588 (2013) 280–287.

[11] Y.G. Jin, H.M. Baek, S.K. Hwang, Y.T. Im, B.C. Jeon, Continuous high strength aluminum bolt manufacturing by the spring-loaded ECAP system, J. Mater. Process. Technol. 212 (2012) 848–855.

[12] K. Edalati, T. Furuta, T. Daio, S. Kuramoto, Z. Horita, High strength and high uniform ductility in a severely deformed iron alloy by lattice softening and multimodal-structure formation, Mater. Res. Lett. 3 (2015) 197–202.

[13] G.J. Fan, H. Choo, P.K. Liaw, E.J. Lavernia, Plastic deformation and fracture of ultrafine-grained Al–Mg alloys with a bimodal grain size distribution, Acta Mater. 54 (2006) 1759–1766.

[14] B.Q. Han, J.Y. Huang, E.J. Zhu, E.J. Lavernia, Strain rate dependence of properties of cryomilled bimodal 5083 Al alloys, Acta Mater. 54 (2006) 3015–3024.

[15] Y. Wang, M. Chen, F. Zhou, E. Ma, High tensile ductility in a nanostructured metal, Nature 419 (2002) 912–915.

[16] S. Cheng, Y.T. Zhao, E. Zhu, Optimizing the strength and ductility of fine structured 2024 Al alloy by nano-precipitation, Acta Mater. 55 (2007) 5822–5832.

[17] M. Hockauf, L.W. Meyer, B. Zillman, M. Hietschold, S. Schultze, L. Krueger, Simultaneous improvement of strength and ductility of Al–Mg–Si alloys by combining equal-channel angular extrusion with subsequent high-temperature short-time aging, Mater. Sci. Eng. A 503 (2009) 167–171.

[18] P.E. Armstrong, J.E. Hockett, O.D. Sherby, Large strain multidirectional deformation of 1100 aluminum at 300 K, J. Mech. Phys. Solids 30 (1982) 37–58.

[19] R.Z. Valiev, R.K. Islamgaliev, I.V. Alexandrov, Bulk nanostructured materials from severe plastic deformation, Prog. Mater. Sci. 45 (2000) 103–189.

[20] Y. Iwahashi, Z. Horita, M. Nemoto, T.G. Langdon, Principle of equal-channel angular pressing for the processing of ultra-fine grained materials, Scr. Mater. 35 (1996) 143–146.

[21] I.J. Beyerlein, D.J. Alexander, C.N. Tomé, Plastic anisotropy in aluminum and copper pre-strained by equal channel angular extrusion, J. Mater. Sci. 42 (2007) 1733–1750.

[22] E.A. El-Danaf, M.S. Soliman, A.A. Almajid, M.M. El-Rayes, Enhancement of mechanical properties and grain size refinement of commercial purity aluminum 1050 processed by ECAP, Mater. Sci. Eng. A 458 (2007) 226–234.

[23] A. Kundu, R. Kapoor, R. Tewari, J.K. Chakravartty, Severe plastic deformation of copper using multiple compression in a channel die, Scr. Mater. 58 (2008) 235–238.

[24] T. Lee, K. Park, D.J. Lee, J. Jeong, S.H. Oh, H.S. Kim, C.H. Park, C.S. Lee, Microstructural evolution and strain-hardening behavior of multi-pass caliber-rolled Ti–13Nb–13Zr, Mater. Sci. ENG A 648 (2015) 359–366.

Materials Letters 227 (2018) 149–153

Contents lists available at ScienceDirect

Materials Letters

journal homepage: www.elsevier.com/locate/mlblue

Featured Letter

Microstructural evolution in the low strain amplitude multi-axial compression (LSA-MAC) after equal channel equal pressing (ECAP) of aluminum

Cleber Granato de Faria [a], Natanael Geraldo e Silva Almeida [a], Franco de Castro Bubani [b], Karla Balzuweit [c], Maria Teresa Paulino Aguilar [d], Paulo Roberto Cetlin [e,*]

[a] Graduate Program in Metallurgical, Materials and Mining Engineering, UFMG, Brazil
[b] CAB(CONICET) and Universidad Nacional de Cuyo, Argentina
[c] Dept. of Physics, UFMG, Brazil
[d] Dept of Construction and Materials, UFMG, Brazil
[e] Dept of Mechanical Engineering, UFMG, Brazil

ARTICLE INFO

Article history:
Received 22 April 2018
Received in revised form 9 May 2018
Accepted 11 May 2018

Keywords:
Metals and alloys
Equal Channel Angular Pressing (ECAP)
Low strain amplitude multi-axial compression (LSA-MAC)
Severe Plastic Deformation (SPD)
Work hardening
Microstructures

ABSTRACT

Low strain amplitude multi-axial compression (LSA-MAC) increases the work hardening capacity and uniform ductility of Aluminum after Severe Plastic Deformation (SPD) through Equal Channel Angular Pressing (ECAP). The mechanisms associated with this processing after ECAP are analyzed. LSA-MAC after 1 ECAP pass in Aluminum softens the material and is connected to the stabilization of the dislocation structures induced by ECAP into a configuration displaying an increased fraction of High Angle Grain Boundaries (HAGB). This occurs for a lower total imposed strain than that through a sequence of high strain ECAP passes or high strain amplitude multi-axial compression (HAS-MAC).

1. Introduction

The production of ultrafine-grained (UFG), high strength metals, through Severe Plastic Deformation (SPD) usually employs Equal Channel Angular Pressing (ECAP), High Pressure Torsion (HPT) or High Strain Amplitude ($\Delta\varepsilon$) Multi-Axial Compression (HSA-MAC, $\Delta\varepsilon \approx 0.5$–$0.8$), [1] also widely known as Multi-Directional Forging (MDF) [2]. UFG materials exhibit low or negative work hardening rate and a low tensile uniform elongation after processing. Microstructural changes in the material before SPD have been developed for increasing their post-SPD low work hardening capacity [3]. A recent study by the present authors [4] showed that Low Strain Amplitude Multi-Axial Compression (LSA-MAC, $\Delta\varepsilon = 0.075$) after ECAP led to an increase in the work hardening capacity of aluminum; this is simpler than pre-SPD microstructural manipulations and can be used for all materials. The present objective is to analyze the microstructural aspects connected to this new procedure. The results indicate that the effects of LSA-MAC after ECAP are associated with the stabilization of the dislocation structures after a much lower total strain than that observed in the usual SPD techniques.

2. Experimental

As-cast 1070 Aluminum specimens underwent: 1 ECAP pass, annealing, another ECAP pass, LSA-MAC (12 compressions, $\Delta\varepsilon = 0.075$) and simple compression. Detailed experimental procedures have been described elsewhere [4]. The material was evaluated in the following conditions: (i) as-cast, 1 ECAP pass and annealed (**An**) (ii) annealed and 1 ECAP pass (**An+ECAP**) (iii) annealed, 1 ECAP pass and LSA-MAC (**An+ECAP+LSA-MAC**) (iv) annealed, 1 ECAP pass, LSA-MAC and compression (**An+ECAP+LSA-MAC +COMP**). The analyses involved microhardness testing, Electron Backscattered Diffraction (EBSD) and Transmission Electron Microscopy (TEM) in the specimen cross-section orthogonal to (i) the extrusion direction for **An** and **An+ECAP**, (ii) the first compressed direction for the **An+ECAP+LSA-MAC** and (iii) the compression direction for the **An+ECAP+LSA-MAC+COMP**. Vickers microhardness employed a Mitutoyo MVK-H1 with a 500 g load for 15 s;

* Corresponding author.
E-mail address: pcetlin@gmail.com (P.R. Cetlin).

https://doi.org/10.1016/j.matlet.2018.05.054
0167-577X/

surface preparation involved initial 600 mesh paper, electrolytic polishing (700 ml C_2H_5OH, 120 ml distilled H_2O, 100 ml $C_4H_9OC_2H_4OH$, 68 ml 70% $HClO_4$ at 35 V for 45 s and a stainless steel cathode). 20 measurements were taken at evenly distributed points in the specimen section. EBSD and TEM were performed in the central part of the above mentioned cross-sections. At least 3 different areas were analyzed for each processing condition; since no remarkable differences were observed for these different areas, one of them was chosen as a typical one for the present paper. TEM employed a Tecnai G2-20 SuperTwin FEI-200 kV (UFMG) or a Philips CM200 Ultratwin–200 kV (Bariloche); specimens were ground to a thickness of 100 μm, punched into 3 mm diameter discs and perforated with a double jet TENUPOL 5 using a 30% nitric acid–methanol solution at 243 K. EBSD specimens were prepared similarly to those for microhardness. A Quanta FEG 3D FEI SEM with a Bruker QUANTAX EBSD analysis system was utilized. Data were processed with the Bruker Esprit 2 software. Detection of neighboring grains was set at a disorientation angle of 2°. For the large grained **An** specimen the area was 30820 μm^2 and step size 270 nm; for the other conditions, the area was 4802 μm^2 and step size 62 nm. ~98.5% and ~90% of the points were indexed for the **An** specimen and for the other specimens, respectively. Noise elimination completed the absent indexing for some points, through an averaging from neighboring points.

3. Results and discussion

The average microhardness for the various conditions were: **An**: 21.2 ± 1.7HV, **An+ECAP**: 45.3 ± 2.9HV, **An+ECAP+LSA-MAC**: 36.5 ± 1.8HV, **An+ECAP+LSA-MAC+COMP**: 40.9 ± 2.0HV. LSA-MAC after the ECAP softens the material, whereas the final compression step hardens it again, in line with a previous report [4].

Fig. 1 displays the Orientation Imaging Microscopy (OIM) results for the conditions: (a) **An**, (b) **An+ECAP**, (c) **An+ECAP+LSA-MAC** and (d) **An+ECAP+LSA-MAC+COMP**. The **An** grains (Fig. 1a) are approximately equiaxed and single colored. The **An+ECAP** condition (Fig. 1b) exhibits large and small elongated grains; the former correspond to the original **An** grains and display color hues, connected to regions with small disorientations, indicating the presence of dislocation cells/subgrains. The additional strain imposed by LSA-MAC after ECAP increases the fraction of areas with small elongated grains (Fig. 1c), often fragmented along their lengths. LSA-MAC caused a fast evolution of initial grains towards equiaxed UFGs due to the variation in the shearing planes associated with the changes in the compression direction [5], similarly to the Bc route in ECAP [6]. The microstructure for the **An+ECAP+LSA-MAC+COMP** condition (Fig. 1d) displays color hues, similarly to the situation after ECAP, indicating the presence of cell/subgrains.

Fig. 2 displays the grain boundary characteristics and disorientation distributions for the conditions, respectively: (a and b) **An**, (c and d) **An+ECAP**, (e and f) **An+ECAP+LSA-MAC** and (g and h) **An+ECAP+LSA-MAC+COMP**. Comparing Fig. 2a and b with Fig. 2c and d indicates that ECAP refined the grains, displaying a predominance of grain disorientations in the range of 2° to 5° (0.637). ECAP also leads to a fraction of 0.866 LAGB (disorientation angles < 15°), similarly to reports in the literature [7,8]. Fig. 2e and f show that LSA-MAC decreased the fraction of grain boundaries with disorientations in the range of 2–5° (0.639 after ECAP, 0.496 after LSA-MAC), coupled to an increase in the fraction of HAGBs (grain disorientation >15°) from 0.134 after ECAP to 0.251 after LSA-MAC. Compression after ECAP+LSA-MAC is connected to a grain disorientation distribution similar to that after ECAP (Fig. 2g and h, HAGB fraction of 0.123), reverting the tendency of increased HAGB fraction caused by LSA-MAC.

Fig. 3 displays TEM images for the conditions: (a and b) **An+ECAP**, (c and d) **An+ECAP+LSA-MAC** and (e and f) **An+ECAP+LSA-MAC+COMP**. **An+ECAP** material displays elongated and equiaxed grains with internal dislocations (Fig. 3a and b), similarly

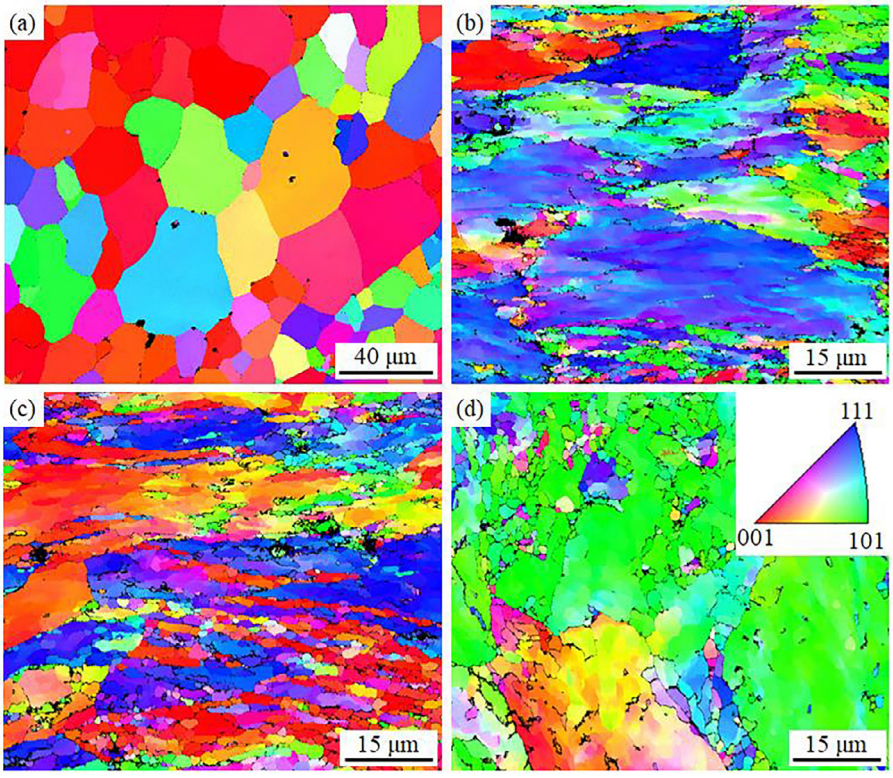

Fig. 1. OIM images for specimens in the conditions: (a) **An**, (b) **An+ECAP**, (c) **An+ECAP+LSA-MAC** and (d) **An+ECAP+LSA-MAC+COMP**.

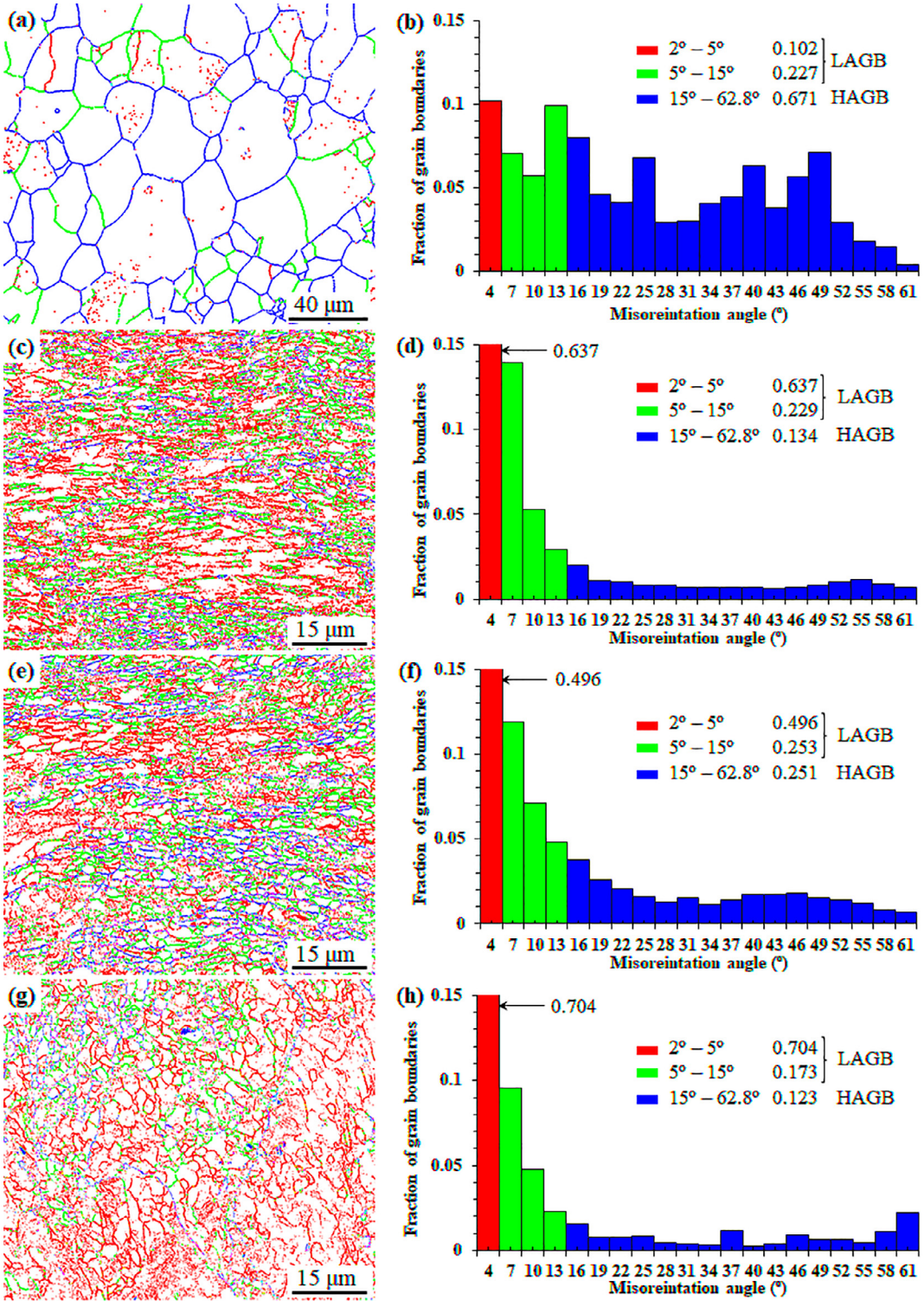

Fig. 2. Grain boundary characteristics and grain disorientation distributions for specimens: (a and b) **An**, (c and d) **An+ECAP**, (e and f) **An+ECAP+LSA-MAC** and (g and h) **An +ECAP+LSA-MAC+COMP**.

to the literature [6]. The grains for the **An+ECAP+LSA-MAC** condition (Fig. 3e and f) are more equiaxed and somewhat smaller than those after **An+ECAP**; displaying intragranular dislocation structures (see the lower right corner, Fig. 3c). Compression after LSA-MAC (**An+ECAP+LSA-MAC+COMP**, Fig. 3e and f) lead to grain sizes somewhat larger than for **An+ECAP+LSA-MAC** (Fig. 3c and d), but without any remarkable differences.

SPD initially forms dislocation tangles and cell walls; that thin and evolve into more stable and lower energy dislocation configurations such as HAGBs [9] as strain rises. This is observed in Aluminum after 4 ECAP passes [10] and after 6 high strain amplitude Multi-axial compression (HSA-MAC) cycles with strain amplitude $\Delta\varepsilon = 0.80$ [11]. The strength of Copper decreases after more than 4 ECAP passes stabilizes up to 16 ECAP passes [12]. This is also

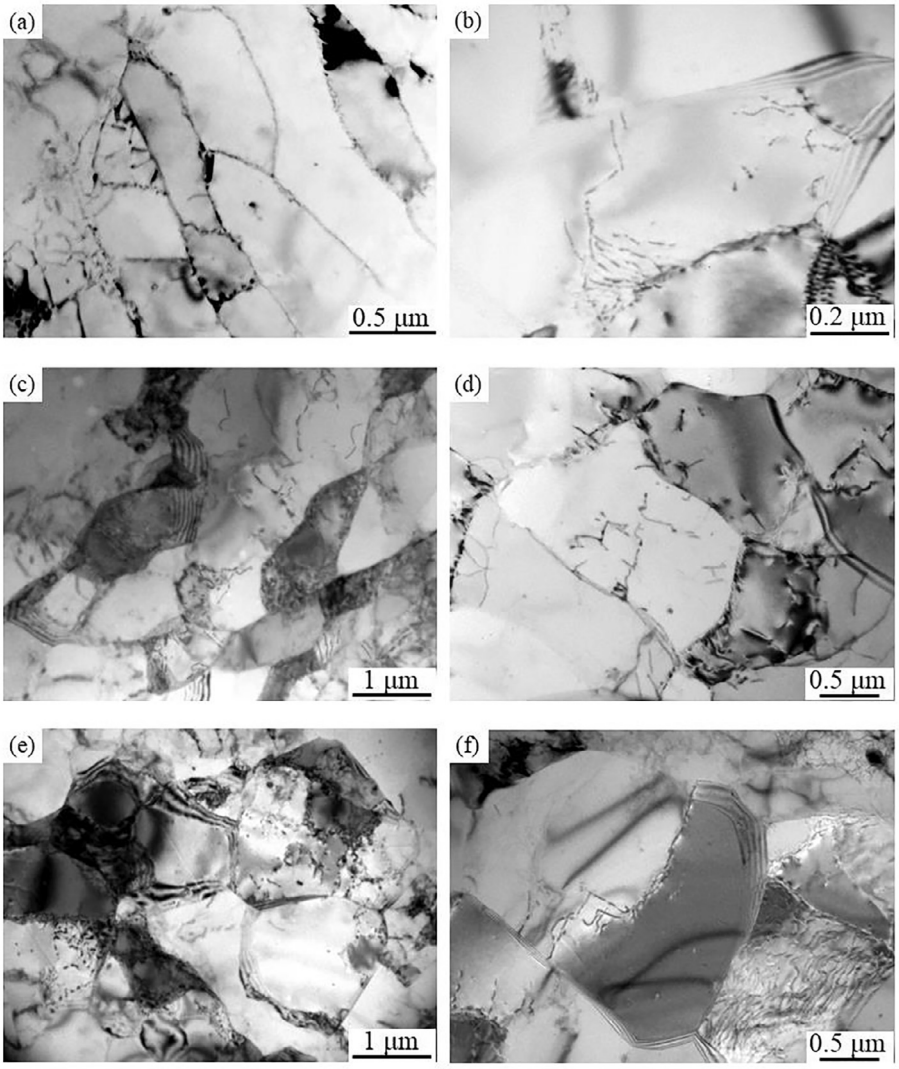

Fig. 3. TEM images for the following conditions: (a and b) **An+ECAP**, (c and d) **An+ECAP+LSA-MAC** and (e and f) **An+ECAP+LSA-MAC+COMP**.

reported for the compression in the transversal direction of Copper after ECAP and Aluminum after 2 ECAP passes [10]. Softening also occurs in Copper [13] and Aluminum [11] in plane strain HSA-MAC after strains of ~4–5, both for a strain amplitude $\Delta\varepsilon = 0.8$. Data for Copper show that, as the number of ECAP passes is raised up to 16, grain size decreases up to 1–2 ECAP passes, followed by grain size stabilization; HAGB/unit area increases up to about 12 passes and slowly decreases up to the 16th pass. Dislocation density rises up to the 4th pass and slowly decreases and stabilizes up to the 16th pass [14].

The present results show that a straining of 1.15 by ECAP followed by LSA-MAC with a total strain of 0.9 (12 steps, $\Delta\varepsilon = 0.075$), totaling a strain of 2.05, led to an HAGB fraction of 0.251, similarly to that for an ECAP strain of ~3 in Al 99,99% [7] and ~4 in Al 1%Mg [8], and to a strain ~4.6 in the HSA-MAC of Aluminum [11] and to a decrease in the material hardness. ECAP **+**LSA-MAC causes effects similar to those described above for Copper [13,14] and Aluminum [11], for a much lower total strain than those reported in the literature. The monotonic compression after ECAP**+**LSA-MAC interrupted the increase in the HAGB fraction caused by LSA-MAC after ECAP and reversed the evolution of this fraction.

4. Conclusions

SPD through ECAP and high strain amplitude multi-axial compression (HSA-MAC, $\Delta\varepsilon \approx 0.5–0.8$) stabilizes the dislocation structures after a large total strain and number of deformation steps.

Low strain amplitude multi-axial compression (LSA-MAC, $\Delta\varepsilon = 0.075$) after ECAP accelerates, in terms of a lowered total imposed strain, the stabilization of the dislocation structures into lower energy arrangements, leading to softening and increased work hardening capacity of the material for further monotonic straining.

Acknowledgments

The authors are grateful for the financial support of the Brazilian Education Ministry, through the CAPES/PROEX and PROF programs of the Graduate Program in Metallurgical and Materials Engineering at UFMG and of MCTI/CNPq and FAPEMIG.

References

[1] R.Z. Valiev, R.K. Islamgaliev, I.V. Alexandrov, Bulk nanostructured materials from severe plastic deformation, Prog. Mater. Sci. 45 (2000) 103–189.

[2] Y. Estrin, A. Vinogradov, Extreme grain refinement by severe plastic deformation: a wealth of challenging science, Acta Mater. 61 (2013) 782–817.
[3] I. Sabirov, M.Y. Murashkin, R.Z. Valiev, Nanostructured aluminium alloys produced by severe plastic deformation: New horizons in development, Mater. Sci. Eng. A 560 (2013) 1–24.
[4] C.G. Faria, N.G.S. Almeida, M.T.P. Aguilar, P.R. Cetlin, Increasing the work hardening capacity of equal channel angular pressed (ECAPed) aluminum through multi-axial compression (MAC), Mater. Lett. 174 (2016) 153–156.
[5] T. Sakai, H. Miura, X. Yang, Ultrafine grain formation in face centered cubic metals during severe plastic deformation, Mater. Sci. Eng. A 499 (2009) 2–6.
[6] T.G. Langdon, The principles of grain refinement in equal-channel angular pressing, Mater. Sci. Eng. A 46 (2007) 3–11.
[7] M. Kawasaki, Z. Horita, T.G. Langdon, Microstructural evolution in high purity aluminum processed by ECAP, Mater. Sci. Eng. 524 (2009) 143–150.
[8] C. Xu, Z. Horita, T.G. Langdon, Microstructural evolution in an aluminum solid solution alloy processed by ECAP, Mater. Sci. Eng. A 528 (2011) 6059–6065.
[9] R.Z. Valiev, Y.V. Ivanisenko, E.F. Rauch, B. Baudelet, Structure and deformaton behaviour of Armco iron subjected to severe plastic deformation, Acta Mater. 44 (1996) 4705–4712.
[10] I.J. Beyerlein, D.J. Alexander, C.N. Tomé, Plastic anisotropy in aluminum and copper pre-strained by equal channel angular extrusion, J. Mater. Sci. 42 (2007) 1733–1750.
[11] R. Kapoor, A. Sarkar, R. Yogi, S.K. Shekhawat, I. Samajdar, J.K. Chakravartty, Softening of Al during multi-axial forging in a channel die, Mater. Sci. Eng. A 560 (2013) 404–412.
[12] F. Dalla Torre, R. Lapovok, J. Sandlin, P.F. Thomson, C.H.J. Davies, E.V. Pereloma, Microstructures and properties of copper processed by equal channel angular extrusion for 1–16 passes, Acta Mater. 52 (2004) 4819–4832.
[13] A. Kundu, R. Kapoor, R. Tewari, J.K. Chakravartty, Severe plastic deformation of copper using multiple compression in a channel die, Scr. Mater. 58 (2008) 235–238.
[14] H.J. Maier, P. Gabor, N. Gupta, I. Karaman, M. Haouaoui, Cyclic stress-strain response of ultrafine grained copper, Int. J. Fatigue 28 (2006) 243–250.